Supporting central nervous system neuroprotection and remyelination by specific TLR4 antagonism

Beatriz Fernández-Gómez[1,2,3], Miguel A. Marchena[1,4], David Piñeiro[2], Yolanda Laó[1], Gloria Valencia[1], Sonia Nocera[1], Rocío Benítez-Fernández[1], Paula Gómez-Martín[1], Ana M. Castaño-León[5], Alfonso Lagares[5], Macarena Hernández-Jiménez[2] & Fernando de Castro[1#].

[1] Instituto Cajal-CSIC, Avda. Dr. Arce 37, Madrid, Spain.

[2] AptaTargets SL, Avda, Cardenal Herrera Oria 298, Madrid, Spain.

[3] PhD Program in Neuroscience, Autónoma de Madrid University-Cajal Institute, Madrid, Spain

[4] Departamento de Medicina, Facultad de Ciencias, Biomédicas y de la Salud, Universidad Europea de Madrid, Villaviciosa de Odón, Spain.

[5] Servicio de Neurocirugía, Hospital 12 de Octubre, Avda. de Córdoba s/n, Madrid, Spain.

#Corresponding author

fdecastro@cajal.csic.es

+34 915854650

ABSTRACT

ApTOLL is an aptamer specifically designed to antagonize toll-like receptor 4 (TLR4), which is involved in the innate immunity that promotes inflammatory responses in several diseases, including multiple sclerosis (MS). MS is a chronic, immune, demyelinating and neurodegenerative disease of the central nervous system that represents the second most important cause of neurological disability in young adults. The drugs currently available to treat this disease are immunomodulators and, to date, there are no therapeutic remyelinating drugs available to manage MS. In this study, we show that TLR4 is located in *post-mortem* cortical lesions of MS patients and as a result, we evaluated the effect of its inhibition by ApTOLL in two different animal models of MS, that of experimental autoimmune encephalomyelitis (EAE) and the cuprizone model. ApTOLL administration ameliorated the clinical symptomatology of the affected mice, which was associated with better preservation and restoration of myelin and oligodendrocytes in the demyelinated lesions of these animals. This revealed not only an immunomodulatory but also a remyelinating effect of the treatment with ApTOLL which was corroborated on purified cultures of rodent and adult human oligodendrocyte precursor cells (OPCs). In summary, the molecular nature of ApTOLL and its mechanism of action strongly supports its further study and use in novel strategies to treat MS and eventually, other demyelinating diseases.

Keywords: Aptamer, ApTOLL, Myelin, immunomodulatory, Oligodendrocyte, TLR4.

INTRODUCTION

Multiple sclerosis (MS) is a chronic, neurodegenerative, inflammatory and autoimmune disease of the central nervous system (CNS) characterized by the appearance of demyelinating lesions. It represents the leading cause of non-traumatic disability in young adults, first displaying clinically signs around the age of 20-40 years [52]. As in other primary demyelinating diseases, the main pathophysiological feature of MS is the loss of oligodendrocytes and myelin in the CNS, both in the white (WM) and gray matter (GM) [67]. This process is also associated with the activation of macrophages and microglia, the resident innate immune cells in the CNS, causing a background of inflammatory reactions [2, 35]. For successful spontaneous remyelination after damage, new mature myelin-forming oligodendrocytes must be generated, which mainly depends on the ability of endogenous OPCs to migrate to lesions sites and differentiate [11, 17, 64]. Although it is known that microglia can promote remyelination through the clearance of myelin debris, the secretion of growth factors and cytokines, and modulation of the extracellular matrix, their chronic activation contributes to the progression of neurodegeneration through the release of multiple neurotoxic factors like tumor necrosis factor-α, nitric oxide or reactive oxygen species [4, 39]. The treatments currently approved for the clinical management of MS are based on the prescription of immunosuppressive and immunomodulatory agents, although there is still no approved drug capable of inducing disease-reversing remyelination [20, 34]. The search for the latter is an important challenge for modern neurology, particularly since the first clinical trial showed positive effects of such an approach [21]. The experimental autoimmune encephalomyelitis (EAE) is the most frequently used animal model to study MS since it induces a variety of immunopathological and neuropathological events that approximate closely to the key features of the relapsing-remitting variety of MS (RRMS) [10]. Furthermore, in other models like the cuprizone model, demyelination and remyelination processes can be studied without the intervention of the immune system [23].

Toll-like receptors (TLRs) are a family of receptors that participate in innate immunity, stimulating a wide variety of inflammatory responses [46]. Specifically, TLR4 has been implicated in several pathologies with a significant inflammatory component, including MS [7, 32, 74]. TLR4 activation increases the expression and nuclear translocation of nuclear transcription factor kappa-B (NF-kB), leading to the release of proinflammatory cytokines like TNF-α, interleukin-1β (IL-1β) or interleukin-6 (IL-6), as well as chemokine and lymphocyte recruitment [38, 40]. In this regard, TLR4 inhibition is known to enhance the survival of oligodendrocytes and OPCs [26, 36, 66]. Therefore, the possibility of

down-regulating immune responses with specific TLR antagonists, inhibiting specific intracellular proteins involved in these signaling pathways, has raised great interest.

This is the case of ApTOLL, a specific innovative antagonist of TLR4 with the potential to achieve an immunomodulatory and anti-inflammatory effect. ApTOLL is a single-stranded DNA aptamer selected using the systemic evolution of ligands by exponential enrichment (SELEX) technology, and its molecular nature and mechanism of action offers a novel strategy to treat diseases with a significant inflammatory component, substantially reducing brain damage [14]. Aptamers offer several advantages over antibodies that make them ideal for future therapeutic applications, such as their high specificity and affinity, and their ease to enter biological compartments given their small size and lack of immunogenicity [76]. Therefore, based on its pharmacokinetic characteristics and its very low level of toxicity, ApTOLL would be suitable for the treatment of different diseases. In fact, ApTOLL has been successfully tested in preclinical models of diseases like ischemic stroke and myocardial infarction, producing an excellent protective effect [14, 60]. In clinical studies, ApTOLL has demonstrated a very good safety profile in a completed First-in-Human clinical trial [27] and it is currently undergoing a Phase Ib/IIa trial (APRIL trial) to determine its safety and biological effect in acute ischemic stroke patients.

In the present work, we are the first to demonstrate the presence of TLR4 in human demyelinating lesions from MS patients, as well as the beneficial effect of this aptamer in different experimental models of MS; EAE and the cuprizone model. These results *in vivo* were corroborated *in vitro*, performing a detailed study of the effects of ApTOLL on primary cultures of OPCs, but also *ex vivo*, by analysis of myelination in cerebellar slices. Together, our study offers proof-of-concept for ApTOLL as a therapeutic agent to treat MS, paving the way to its possible use in combination therapy to produce an immunomodulatory, neuroprotective and neuroreparative effect. Indeed, we expect that in such a scenario ApTOLL will reduce inflammation and demyelination, while improving the survival and replenishment of endogenous OPCs and mature oligodendrocytes, thereby enhancing remyelination.

MATERIALS AND METHODS

Human brain samples. *Post-mortem* cortical brain tissue blocks from human MS patients and controls were obtained from the UK Multiple Sclerosis Tissue Bank. Alternate coronal slices or brain hemispheres were fixed in 4% paraformaldehyde (PFA) for ~2 weeks and were then cryoprotected in 30% sucrose for ~1 week and frozen in isopentane precooled on a bed of dry ice. Microtome sections (50 µm) were obtained from all the cortical blocks, containing GM and WM for immunohistochemical analysis [8]. Blocks from MS patients with WM lesions and controls were studied here, from individuals with no history of neuropsychiatric disease in either case (Table 1).

Animals. Female and male C57/BL6 mice (7-weeks-old) were purchased from Charles River Laboratories (Wilmington, MA, USA), while 8-week-old female C57BL/10ScNJ mice (formerly C57BL/10ScCr) that do not express TLR4 (TLR4$^{-/-}$) [57] were purchased from Jackson Laboratory (Bar Harbor, Me, USA) and the colony was maintained at the *Centro de Investigaciones Biológicas Margarita Salas (CIB)-CSIC*. The TLR4$^{-/-}$ animals used in the *in vivo/in vitro* studies were transferred to the animal facility at the *Instituto Cajal*, where the mice were acclimatized for a week in the appropriate environmental conditions with *ad libitum* access to food and water prior to carry out the procedures. Wistar P7 rats from the animal facility of the *Instituto Cajal* were also used in primary cultures. All experimental procedures were performed in accordance with European Council Guidelines (63/2010/EU), and Spanish National and Regional Guidelines for Animal Experimentation and Use of Genetically Modified Organisms (RD 53/2013 and 178/2004, Ley 32/2007 and 9/2003, Decree 320/2010). The generation of the different MS models was approved by the relevant institutional and regional ethics committees CSIC (440/2016, Madrid, Spain).

Induction of active EAE. EAE was induced in female *wild type* (WT) and TLR4$^{-/-}$ mice as described previously [47, 50]. The mice were first anesthetized with 40 µl of an anesthetic/analgesic solution containing Ketamine (40 mg/ml: Anesketin) and Xylazine (2 mg/ml: Rompun) injected intraperitoneally (i.p.). An emulsion of the Myelin Oligodendrocyte Glycoprotein (MOG_{35-55} peptide, 250 µg in a final volume of 200 µl: GenScript) and complete Freund's adjuvant (CFA) containing inactivated *Mycobacterium tuberculosis* (4 mg: BD Biosciences) was introduced subcutaneously into the animal's groin and armpits. Then, pertussis toxin (400 ng/mouse: Sigma-Aldrich) was administered intravenously (i.v.) through the tail vein on the day of immunization and 48h later. The mice were weighed and evaluated double-blind on a daily basis until sacrifice, scoring the animals as follows: 0, asymptomatic; 1, loss of muscle tone throughout the tail; 2, weakness or unilateral partial hind limb paralysis; 3, bilateral paralysis of the hind

limbs; 4, tetraplegia; and 5, death. In all cases, mice were sacrificed ten days after the onset of symptoms. After EAE induction, animals were evaluated on a daily basis and sacrificed 10 days after the onset of clinical symptoms.

ApTOLL treatment. ApTOLL (0.45 mg/kg, 0.91 mg/kg, 1.82 mg/kg or 3.6 mg/kg, diluted in sterile PBS/1mM $MgCl_2$ -vehicle) was administered i.v. to the WT and $TLR4^{-/-}$ mice through a single injection at the onset of the symptoms (defined as a clinical score between 0.5 and 1.5). For the study of the therapeutic window, independent groups were established, and a single 0.91 mg/Kg dose was injected 24h after the onset and at the peak of the symptoms.

Cuprizone-induced model. Male, 8-week-old C57/BL6 mice were randomly separated into three groups: control untreated, ApTOLL-treated, and vehicle treated. While the control animals received a normal diet, the rest of the mice were fed chow containing cuprizone (CPZ, bis (cyclohexanone) oxaldihydrazone: Sigma-Aldrich) at 0.25% (w/w) *ad libitum* for 6 weeks [45], a copper chelator that induces apoptosis of mature oligodendrocytes and that leads to robust demyelination, particularly in the corpus callosum (CC) [23, 58]. The body weight of each mouse was controlled weekly, and ApTOLL or the vehicle alone was also injected i.v. once weekly from the beginning of the experiments to the time of sacrifice. To study CPZ-induced oligodendroglial proliferation, we add EdU (5-ethynyl-2'-deoxyuridine; Invitrogen), a direct measure of de novo DNA synthesis, into the drinking water at 0.2 mg/ml the week before sacrifice.

Motor coordination test (Rotarod). At the end of the 6-week experimental period, the animals were tested on the rotarod to evaluate their locomotor coordination [15]. For training, mice were subjected to pre-test trials the day before, placing them on the rod at constant speed (30 rpm). Each mouse performed the test twice in the same conditions as the pre-test trials and the latency to fall was measured.

Tissue sampling. Animals were sacrificed by i.p. administration of a lethal dose of pentobarbital and they were perfused transcardially with 4% PFA in 0.1M Phosphate Buffer (PB, pH 7.4). The brain and spinal cord were obtained and post-fixed for 4h at room temperature (RT) in 4% PFA. The tissue was cryoprotected by immersion in an increasing sucrose gradient and coronal cryostat sections (20 µm) were obtained on a CM1900 cryostat (Leica).

Eriochrome-cyanine staining. To analyze CNS demyelination, eriochrome-cyanine (EC) staining was performed as described previously [45, 50]. The histological sections were dried for 2h at RT and for 2h at 37 °C, before they were immersed in acetone for 5 min, dried and submerged in the EC solution (Sigma) for 30 min. To differentiate the

samples, iron alum at 5% (w/v) was used for 5–10 min followed by a second differentiation step with borax-ferricyanide solution for 5 min at RT. For conservation, the sections were dehydrated in ethanol solutions of increasing concentration and mounted with mounting medium.

Immunohistochemistry in CNS tissue. In human tissue, TLR4 was detected using diaminobenzidine (DAB). Briefly, the tissue was first pre-treated with 0.3% hydrogen peroxide in methanol for 5 min in order to eliminate endogenous peroxidases. Samples were washed in 0.1M PB and blocked with a solution containing: 1% of normal goat serum (NGS), 0.2% of Triton X-100 in PBS for 1h at RT. After that time, they were incubated with the primary antibody (see Table 2) overnight at RT, washed with PBS and incubated with the secondary antibody (1:1000) for 1:30h at RT. Samples were then washed with PBS and immersed in the solution containing the avidin-biotin-peroxidase complex (Ultra-Sensitive ABC Peroxidase Standard Staining Kit, ThermoFisher) for 30 min at RT. Finally, they were washed with PBS and 0.1% Tris-HCl buffer for 5 min, and peroxidase was revealed with a solution consisting of: 0.02% of 3,3'-diaminobenzidine (Sigma), 0.003% of hydrogen peroxide in 0.2% Tris-HCl buffer. The reaction was controlled under the microscope and stopped by washing the samples with 0.05% of Tris-HCl buffer. Before mounting, the tissue was dehydrated in ethanol solutions of increasing concentration.

To detect antigens present in the spinal cord (SC) of EAE mice and the CC from CPZ-treated animals, sections were first pre-treated with 10% methanol in 0.1M PB at RT for 15 min and after several washes with 0.1M PB and PB saline (PBS), then they were incubated for 1h at RT with blocking solution to avoid non-specific binding: 5% of normal donkey serum (NDS) and 0.02% of Triton X-100 (Sigma-Aldrich) in PBS. The sections were then incubated overnight at 4 °C with the primary antibodies (see Table 2) and after washing, they were probed for 1h at RT with the fluorescent secondary antibodies (1:1000: ThermoFisher). Cell nuclei were stained with Hoechst 33342 (10 µg/mL: Sigma-Aldrich) and finally, the tissue was washed and mounted with Fluoromont® mounting medium (SouthernBiotech). We also used FluoroMyelin Green fluorescent myelin stain (Invitrogen) for the quick and selective labeling of myelin in brain cryosections. As such, the samples were rehydrated with PBS and incubated with the staining solution for 20 min at RT. Subsequently, the sections were rinsed in PBS three times and mounted with Fluoromont®. To visualize cell proliferation, EdU detection cocktail (Click-iT EdU Alexa Fluor 488 HCS assay, Invitrogen) was used according to the manufacturer's instructions.

Primary Oligodendrocytes precursor cell (OPC) cultures. OPCs from the cerebral cortex of P7 Wistar rats and TLR4$^{-/-}$ mice were isolated using Magnetic-Activated Cell

Sorting-MACS (Miltenyi) [12, 48]. First, the animal's brain was extracted and the meninges removed in a Petri dish containing cooled $HBSS^{+/+}$ (Hank's Balanced Salt Solution with Ca^{2+} and Mg^{2+}: Gibco) to maintain their metabolism. According to the manufacturer's instructions, the brain cortices were then mechanically triturated in $HBSS^{-/-}$ and enzymatically digested for 25 min at 37 °C with the enzymes provided in the Neural Tissue Dissociation Kit (P) (Miltenyi) under mild and continuous agitation. After adding the second mix, the tissue was dissociated with a 5 ml pipette. The suspension was passed through 70 µm nylon cell strainer (BD Falcon), centrifuged at 300 g for 10 min and incubated for 25 min at 4°C with the primary antibody from A2B5 (Millipore) and/or O4 hybridoma cells (DSHB: Developmental Studies Hybridoma Bank, Iowa) diluted 1:1 in a Miltenyi wash buffer (MWB – 2 mM sodium pyruvate, 0.5% BSA and 2 mM EDTA adjusted to pH 7.3). After that, cells were washed with MWB and exposed to the secondary rat anti-mouse IgM antibody (anti-mouse IgM microbeads: Miltenyi) for 15 min at 20 µl/10^7 cells. Next, the cell suspensions were washed and passed through a MWB-coated medium-size column (MS, Miltenyi) coupled to a magnet and eluted with Neuromedium (Miltenyi) supplemented with 2% MACS® NeuroBrew-21 w/o vitamin A (Miltenyi), 0.6% Penicillin/Streptomycin (10,000 U/ml penicillin and 10 mg/ml streptomycin: Sigma), glutamine (200 mM, Gibco), D-glucose (25 mM, Normapur) and 10 ng/mL of PDGF-AA (Platelet Derived Growth Factor-AA: Merck) and FGF-2 (Fibroblast Growth Factor-2: Peprotech). Finally, the cells were counted and seeded on coverslips coated with poly-L-Lysine (0.1 mg/ml in borate buffer, pH 8.5: Sigma) and laminin (10 µg/ml in PBS: Sigma). A purity of ~90% was obtained.

Human OPCs were isolated from biopsies of the adult cerebral cortex following surgery of traumatic brain injury patients, obtained from the Neurosurgery Services of the Hospital 12 de Octubre (Madrid), and conserved immediately in Hibernate-A (Gibco) at 4 ºC up to the isolation process. The study was conducted according to the guidelines and the Research Ethics Committee approved protocol of the *Instituto Cajal-CSIC* (440/2016 and 2016/049/CEI3/20160411). To obtain the cells, the same procedure was applied with some modifications. After filtration, the pellet was passed through a 20% Percoll (GE Healthcare) gradient and centrifuged at 800 g for 20 min. The cells were then exposed to a Red Blood Cell Removal Solution (Miltenyi) diluted in ddH_2O for 10 min at 4 ºC. An anti-O4 Microbead antibody (2.5 µl: Miltenyi) was resuspended in 97.5 µl of MWB and used to label up to 10^7 total cells by incubating for 15 min at 4 ºC in the dark with mild agitation. Culture purity was at least 85%.

Viability/survival assay. The viability of the OPCs after the different treatments was tested with a MTT (Thiazolyl blue tetrazolium bromide) assay that measures the mitochondrial

activity of the cells by quantifying the conversion of the tetrazolium salt to its formazan product. Cells were seeded in 96-well plates at a density of 15,000 cells/well in a final volume of 200 µl and treated the day after the culture with ApTOLL (20 nM and 200 nM), the vehicle alone or 5% H_2O_2 as a cell death control. After 24h, MTT (5 mg/ml: Sigma) was added to the plates and the cells were left in the incubator for 4h, after which the medium was removed, DMSO (dimethyl sulfoxide; Invitrogen) was added to dissolve the formazan formed and the absorbance of this solution was measured. Likewise, the survival of OPCs was determined by TUNEL staining (Terminal deoxynucleotidyl transferase dUTP nick end labeling: see [48]. To this end, the cells were seeded in 24-well plates at 30,000 cells/coverslip in a final volume of 500 µl, treated with ApTOLL or the vehicle alone on the following day, and then fixed in 4% PFA after 48h.

Proliferation assay. To analyze OPC proliferation, the cells were seeded, as previously described, at a density of 30,000 cells/coverslip [44, 48] and after 24h, the medium was replaced with medium containing the corresponding treatments and 6h a pulse of BrdU (5-bromo-2-deoxyuridine, 50 µM; Sigma-Aldrich) was given to the neonatal cells. At the end of this time, the medium was refreshed and the cells were fixed with 4% PFA on the following day.

Differentiation assay. Cells were seeded at 30,000 cells/coverslip and 24h later, the medium was replaced with new medium without growth factors (PDGF-AA and FGF-2). The following day the treatments were added and the cells were fixed and immunolabelled at the end of the fifth day *in vitro*.

Immunocytochemistry of *in vitro* cultures. After fixing the cells with 4% PFA, they were washed with PBS and maintained for 1h under shaking in the blocking solution (5% NDS and 0.02% Triton X-100). The cells were then incubated overnight with the corresponding primary antibodies in a humid chamber at 4 °C (Table 2) and after washing they were exposed to the secondary antibodies for 1h at RT in the dark. The nuclei were staining with Hoechst (1:20) for 10 min in the dark and the coverslips were mounted in Immu-mount (ThermoFisher).

To study proliferation, BrdU labelling was performed after Olig2 staining. After washing the cells, they were denatured with HCl 2N for 45 min at RT, washed with borate buffer and blocked for 3h at RT with PBS containing 5% FBS (Fetal Bovine Serum), 0.03% Triton X-100, 0.2% gelatin and 0.2M glycine. They were then incubated overnight at 4 °C with an anti-BrdU rat antibody (Abcam) diluted in blocking solution and after several washes, they were exposed to the secondary antibody for 4h before Hoechst staining. TUNEL staining was performed with the ApoTag Plus Fluorescein *in Situ* Apoptosis kit

(Millipore Merck, Sigma-Aldrich) following the manufacturer's instructions. Briefly, cells were equilibrated with the corresponding buffer and incubated for 1h at 37 °C in 50% Terminal deoxynucleotidyl transferase (Tdt) in reaction buffer. The reaction was stopped and after washing, the coverslips were exposed for 30 min to 47% anti-digoxigenin diluted in blocking buffer. Finally, the standard protocol was applied to label additional markers.

Organotypic cultures of cerebellar slices. Cerebellar slices from neonatal mice were cultured following standard protocols [3, 45, 48]. Mice were decapitated, and their brain and cerebellum were deposited in a Petri dish with $HBSS^{+/+}$ on ice. The cerebellum was separated, immediately placed on a Teflon base and cut automatically into 350 µm slices on a McIlwain Tissue Chopper (Mickle Laboratory Engineering Co. Ltd). Cerebellar parasagittal slices were transferred under sterile conditions to 30 mm diameter MilliCell inserts with a pore size of 0.4 µm (Millipore), placed in a 6-well plate with 1 ml of culture medium consisting of: 25% $HBSS^{+/+}$, 50% BME (Basal Medium Eagle: Gibco), 25% inactivated horse serum (Gibco), 28 mM D-glucose, 1% Penicillin/Streptomycin solution and 0.25 mM Glutamax (Gibco). The medium was refreshed every other day and a demyelinated toxin, lysolecithin (LPC, 0.5 mg/ml: Sigma), was added after 7 days *in vitro* (DIV) for 15h. Subsequently, the medium was removed and the slices were treated with ApTOLL (20 nM) or the vehicle alone in fresh culture medium. The cultures were maintained until 6 days post-lesion (dpl), refreshing the medium and treatment every other day, fixing samples with 4% PFA for 15 min at both 0 dpl as an internal control for the effectiveness of LPC and at 6 dpl. Finally, they were stained for MBP (Myelin Basic Protein), NFH (Neurofilament heavy chain) and Iba1 as described above.

Image and data analysis. Optical images of EC and DAB staining were acquired and mosaics built using the brightfield camera of the THUNDER microscope (LEICA) at 20X and 40X magnification. Fluorescence images of tissue samples were taken on an inverted Leica SP-5 confocal microscope at the Microscopy and Image Analysis Unit of the *Instituto Cajal*. In the EAE model, mosaics of three SC samples were obtained per animal at 40x magnification and at a resolution of 512 x 512 pixels, with a separation between z-planes of 3 µm. Demyelinated areas and MBP/NFH staining were assessed using the ImageJ application, and the cell counts analyzed with the microscopy software for 3D and 4D Imaging (IMARIS). Similarly, the central zone of the CC was evaluated in the CPZ model. Images were acquired with the same confocal microscope at a 40x magnification (for Caspr labeling a 63x objective was used), at a resolution of 1024 x 1024 pixels and with a separation of 0.5 µm between the z-planes. The same parameters were applied for microphotographs of cerebellar slices, including a digital zoom of 1.7.

The quantification of the different markers was performed using ImageJ software. Images of primary cultures were obtained with a Leica AF 6500-7000 microscope (five random photos per coverslip at 20x magnification) and they were counted manually with the LAS X Life Science software. The absorbance for the viability assay was measured with a fluorometer FLUOstar OPTIMA (BMG Labtech) at 595 nm.

Morphometric analysis of microglia. We studied the morphological complexity of microglia to determine their functionality in organotypic slices under inflammatory conditions (exposed to LPC). A minimum of 10 cells per condition were randomly analyzed and processed with the ImageJ software, following the previously published protocol [70]. In summary, for the skeleton analysis the image was first adjusted for brightness/contrast if necessary and processed to remove background noise. It was then converted to a binary image and the AnalyzeSkeleton (2D/3D) plugin was run. The results were obtained from the Branch Information box.

Statistical analysis. The data are expressed as the means ± SEM throughout and they were analyzed with GraphPad (GraphPad Software, La Jolla California USA). First, a D'Agostino & Pearson normality test was passed to check if the values followed a Gaussian distribution. To compare pairs of independent groups, Student's *t*-test was used or a Mann-Whitney U test for non-parametric data. For multiple comparisons, One-Way ANOVA test was carried out in conjunction with the corresponding *post hoc* tests: Tukey's test for parametric samples and Dunn's test for non-parametric samples. The threshold for statistical significance was set at $p < 0.05$ and the results of the analysis were represented in text and figures as: *$p < 0.05$; ** $p < 0.01$; ***$p < 0.001$.

RESULTS

Presence of TLR4$^+$ cells in demyelinating plaques of MS patients

TLR4 has been associated with pathological processes and inflammation, ergo we studied whether TLR4 was dysregulated in the CNS of *post-mortem* samples of MS patients (Table 1). Demyelinating lesions were identified by EC staining and HLA-DR to detect the presence of inflammatory infiltrate (Fig. 1a-b, e-f, i-j). While almost any track of TLR4 staining was detected in the tissue of control patients (Fig. 1c-d), TLR4$^+$ cells were abundant within active (Fig. 1g-h), but just scarce in the core of chronic plaques (Fig. 1k-l) of MS patients. Unfortunately, TLR4 staining just worked with DAB staining but not in immunofluorescence, which did not allow us to perform double-staining to identify the cell types expressing this (data not shown). According to previous studies in similar samples [8, 61], the morphological aspect and distribution of TLR4$^+$-cells in active lesions suggested a net inflammatory predominance (Fig. 1g-h), but in the core of chronic lesions, the very few TLR4$^+$-cells suggested neural phenotypes (i.e: oligodendroglial; Fig. 1k-l). As TLR4 is upregulated in MS brain, we next investigated this in preclinical models of inflammation and demyelination and explore whether antagonized with the innovative aptamer ApTOLL would be beneficial throughout the course of pathology over time, as previously observed in other neurological diseases [14, 60].

ApTOLL treatment reduces EAE severity and demyelination in the spinal cord

In this model of EAE, there is T-cell driven inflammation and demyelination in the spinal cord, modelling the highly inflammatory early phase of MS. The optimal dose of ApTOLL for reduction of clinical score was determined by assessing four different concentrations (0.45 mg/Kg, 0.91 mg/Kg, 1.82 mg/Kg and 3.6 mg/Kg) administered through a single i.v. injection at the onset of EAE symptoms (see Methods section for details). The recovery of the clinical scores reached were significantly lower when the two intermediate doses were used (Supplementary Fig. 1a, online resource). Importantly, the Sham group did not present any pathological manifestations in these studies (data not shown). Histology study showed significantly less demyelination after administration of both the 0.91 and 1.82 mg/kg doses (Supplementary Fig. 1b-c, online resource), although the significantly better preservation of myelin (MBP staining) and axons (NFH staining), as well as the significantly larger proportion of OPCs (PDGFRα immunostaining) with no apparent changes in microglia (Supplementary Fig. 1d-g, online resource), led us to choose the dose of 0.91 mg/kg ApTOLL as optimal for our purposes (as used in the rest of our study). Similarly, we determined the therapeutic window for the single dose of ApTOLL,

at the onset of EAE symptoms, 24h post-onset or at the peak of the symptoms. Although there was a reduction in clinical severity in each of these three treatment groups, the effects of ApTOLL were strongest when it was administered at the onset and 24h post-onset (Supplementary Fig. 2a, online resource). Demyelination was significantly lower in the three groups treated with ApTOLL when compared with the EAE-Veh animals (that received the vehicle alone), although this effect was particularly stronger when this agent was administered at the onset of EAE symptoms (Supplementary Fig. 2b-c, online resource), as it was in general for the rest of the histological parameters studied (Supplementary Fig. 2d-g, online resource). Together, our results suggest that a single dose of 0.91 mg/kg ApTOLL administered as soon as the mice presented symptoms was effective to protect the CNS from the demyelinating insult and that there was at least some evidence that spontaneous remyelination may also have been promoted.

With this selected dose, differences between the EAE-Veh and EAE-ApTOLL-treated group were observed from the beginning of the treatment, as there was a clear reduction in the slope of the curve and the disease scores obtained for the latter were significantly lower from day 4 onwards (Fig. 2a). The EAE-ApTOLL treated mice also showed a high recovery rate at the end-point compared to both the vehicle mice (67.2 ± 2.4%) and their own clinical scores at the peak of the disease (ApTOLL recovery at the end-point vs. peak: 61.8 ± 4.9%). In accordance with these results, EAE-ApTOLL-treated animals had fewer and relatively smaller demyelinated lesions in the WM (mainly ventro-lateral) than the EAE-Veh mice (Fig. 2b). Indeed, the total demyelination diminished significantly (by 75%) in the animals that received ApTOLL (Fig. 2c). The areas of well-preserved myelin and neurofilaments (expressing MBP and NFH, respectively) were significantly larger in the EAE-ApTOLL-treated animals than in those EAE-Veh animals (Fig. 2d-f). Although a significant increase in the number of cells in the oligodendroglial lineage (Olig2^{+} cells) was observed following ApTOLL treatment, the effects were particularly notable for OPCs (Olig2^{+}/PDGFRα^{+} cells) and mature oligodendrocytes (Olig2^{+}/CC1^{+} cells: Fig. 2d-g).

ApTOLL effects in EAE are due to TLR4-specific antagonism

ApTOLL is known to selectively antagonize TLR4 in a murine model of brain ischemia [14], which suggests it crosses the blood brain barrier (BBB). To assess the mechanism of action of ApTOLL in our demyelinating models, we induced EAE in *TLR4*$^{-/-}$ mice. In our present study, the *TLR4*$^{-/-}$ mice were susceptible to this disease (91.7% incidence vs 47.0% in *WT* mice), reaching a mean maximum clinical score of 2.5 (± 0.2) 5 days after

the onset of symptoms and with a mean disease onset at 11 dpI. While ApTOLL treatment in WTs was effective with a 67% recovery rate, no effects of this antagonist were evident in the TLR4$^{-/-}$ treated and untreated mice (Fig. 3a). Regarding the number and proportion of the total demyelinated areas in the WM, no noticeable differences were found between the *TLR4*$^{-/-}$ mutants and the WT EAE-Veh mice, even though the WT EAE-ApTOLL group developed significantly fewer and smaller lesions, as seen previously (Fig. 3b, c). This was also reflected in the analysis of the markers of myelin (MBP: Fig. 3d, e) and neurofilaments (NFH: Fig. 3d, f). Regarding the dynamics of the oligodendroglial populations, no effects were seen in the *TLR4*$^{-/-}$ animals. Although there were more OPCs than in the WT EAE-Veh mice (Fig. 3g, h), no differences were found in the mature oligodendrocytes in the TLR4$^{-/-}$ mice, (Fig. 3g, i), suggesting that the effect of ApTOLL on oligodendrocytes also involves TLR4.

TLR4 is mostly expressed by microglia and its blockade decreases inflammation in EAE mice

As inflammation is one of the main characteristics of MS and due to the central role of TLR4 in the activation of microglia, we determined the presence of microglial cells in the SC of EAE mice that had been injected with ApTOLL at the onset of symptoms. A significant decrease to approximately half the number of these inflammatory cells was detected, especially in the lesion areas (Fig. 4a, b). Moreover, this process seemed to be favored by the shift of these cells towards anti-inflammatory phenotypes, as evident through their morphology (greater number and length of branches) [9, 24, 54], after exposure to a demyelinating insult and the subsequent treatment with ApTOLL (Supplementary Fig. 3, online resource). Similarly, the quantitative analysis of demyelinating lesions showed a significant reduction in the density of TLR4-labelled cells after treatment with ApTOLL (Fig. 4a, c), as well as in those cells co-expressing both markers (Iba1^{+}/TLR4^{+} cells: Fig. 4a, d), with a direct correlation between the expression of this receptor and the number of microglial cells (Fig. 4e).

ApTOLL also promotes remyelination in the mouse cuprizone model of MS

To better evaluate the effects of ApTOLL on oligodendroglial biology, we took advantage of the CPZ *in vivo* model as this copper chelator induces reversible demyelination in the CNS, particularly in the CC [33]. Mice were maintained on a CPZ diet for 6 weeks with a weekly dose of ApTOLL throughout (see Materials and Methods for details; Fig. 5a). Analysis of the proliferation of OPCs at the end of week 3 by quantifying the co-

immunolabelled Olig2^{+}EdU^{+} cells, revealed an enhancement in the proportion of double-staining cells in ApTOLL-treated animals (Control 5.0% ± 1.8, Cpz-Veh 6.2% ± 2.2, Cpz-ApTOLL 20.3% ± 5,7; Student's *t*-test Cpz-Veh vs. Cpz-ApTOLL: p = 0.058), suggesting enhanced OPC proliferation [23]. After 6 weeks, when the peak of demyelination occurs, we examined the motor coordination and balance of the mice in a rotarod test and the latency to fall of the CPZ-Veh mice decreased significantly with respect the control mice. Administration of ApTOLL to the CPZ animals improved their motor function, these closely resembling the control animals (Fig. 5b). In agreement with previous reports [22, 43, 65], a six-week CPZ treatment induced almost complete loss of myelin in the CC in the CPZ-Veh group, while weekly ApTOLL injection partially but significantly protected this tissue against demyelination (Fig. 5c, d). The role of this compound in the preservation of mature myelinated axons was also suggested by the number of nodes of Ranvier: while this was markedly reduced in CPZ-Veh demyelinated animals, ApTOLL treatment doubled their number, although remaining significantly far from the control group (Fig. 5c, e). In addition, the number of OPCs recovered significantly after ApTOLL administration, as did that of mature oligodendrocytes, although while double the OPC numbers in CPZ-Veh mice they remained lower (about one quarter) than in the control mice (Fig. 5c, f-g).

ApTOLL treatment enhances OPC proliferation and differentiation *in vitro* without affecting their survival

The *in vivo* data obtained previously in these animal models of MS suggest that ApTOLL affects different pathogenic aspects, maybe including the promotion of spontaneous remyelination (Figs. 2, 4 and 5). To further elucidate whether ApTOLL exerts a direct effect on OPCs, we verified the expression of TLR4 in these cells: in the CNS of adult mice, TLR4 colocalized with markers of the entire oligodendroglial lineage (Olig2) and specific markers of OPCs (PDGFRα; Fig. 6a). This strongly suggest that ApTOLL would also directly modulate OPC biology.

We analyzed the survival, proliferation and differentiation of these cells in purified primary cultures after they were isolated from the cerebral cortex of neonatal rats and exposed to the aptamer at two different concentrations (20 nM and 200 nM, as tested previously: [14]). Neither OPC viability in MTT assays (data not shown) nor their survival in TUNEL assays (Fig. 6b-c) were affected by ApTOLL, however exposure to this aptamer did significantly induce OPC proliferation (Fig. 6d-e). Moreover, to explore the role of the aptamer in the maturation of OPCs towards myelinating phenotypes and their myelin

production, we maintained cells in culture for 5 days under the different experimental conditions. Exposure to ApTOLL produced a significant increase not only in the number of mature oligodendrocytes expressing the MBP marker (Fig. 6f-g) but also, in the area occupied by this antibody relative to the control OPCs (MBP^+ area in Veh 4711 ± 1402 μm^2, in ApTOLL [20 nM] 8082 ± 757 μm^2 and in ApTOLL [200 nM] 9871 ± 1415 μm^2: One-Way ANOVA Dunn's *post hoc* test Veh vs. ApTOLL [20 and 200 nM] $p < 0.001$). Similar results were obtained in murine OPCs (data not shown). To probe if these were effects mediated by TLR4, we studied OPCs isolated from the brain cortex of neonatal $TLR4^{-/-}$ mice and no differences were detected following exposure to ApTOLL or the vehicle alone in any of the different assays performed to assay OPC survival, proliferation or differentiation (Supplementary Fig. 4, online resource). Accordingly, we concluded that ApTOLL exerts a direct promyelinating role *in vitro* and that this seems to be driven through TLR4 expressed by oligodendroglia.

ApTOLL promotes remyelination *ex vivo*

To study the impact of ApTOLL on myelin regeneration after a demyelinating insult, *ex vivo* organotypic cerebellar slice cultures were prepared from neonatal mice and tissue damage was provoked with LPC, a membrane-disrupting chemical that provokes rapid loss of myelin and oligodendrocytes [3, 48] (Fig. 7a). Demyelination with LPC was confirmed after being removed from the medium with a 55-60% reduction in both the amount of myelin and its co-localization with neurofilaments. To study the remyelinating effect of the aptamer, we maintained the slices for 6 dpl and increased myelin production was evident in LPC slices that received ApTOLL than in those that received the vehicle alone (Fig. 7b, c). Moreover, treatment with ApTOLL resulted in a significantly higher proportion of remyelinated axons than when they were exposed to the vehicle alone (Fig. 7b, d), the latter only showing a 22% increase over the control at 0 dpl (LPC+Control 22.6% ± 3.0, LPC+Veh 27.6% ± 6.8: Student's *t*-test $p = 0.45$), whereas exposure to ApTOLL produced a 130% increase (LPC+Control 22.6% ± 3.0, LPC+ApTOLL 51.8% ± 6.7: Student's *t*-test $p < 0.001$). These data confirmed the ability of ApTOLL to enhance new myelin generation and promote the formation of new sheaths around axons that had been previously demyelinated.

ApTOLL enhances the maturation of human adult OPCs towards myelinating phenotypes and increases myelin production

Based on the data obtained from rat OPCs *in vitro*, we determined whether ApTOLL exerted a promyelinating effect in primary cultures of adult human OPCs isolated from non-tumor biopsies of the adult cerebral cortex (see Materials and Methods). As described previously [6, 44, 45], it was necessary to maintain these cells for at least 15 DIV to differentiate them. Exposure to ApTOLL (20 nM) gave rise to significantly more mature oligodendrocytes ($CC1^+$) than when the OPCs were cultured in control conditions, and these differences were even more pronounced when 200 nM ApTOLL was used (Fig. 8a, b). However, both these treatments gave similar results in terms of the myelin proteins generated by these mature oligodendrocytes (measured as MBP^+ area) with respect to the total number of cells quantified in each field (Fig. 8a, c). Together, these results show that as seen with rodent cells, ApTOLL may have a direct effect on promoting the production of proteins needed for myelin formation by human adult OPCs and they suggest that ApTOLL may be a suitable agent to directly promote effective remyelination in MS in addition to its anti-inflammatory activities.

DISCUSSION

The contribution of the inflammatory-immunological component to MS pathogenesis has been extensively demonstrated, in which TLRs (including TLR4) play important roles [1, 19, 53, 73]. Up to our knowledge, our present work is the first to identify this receptor in human MS demyelinating lesions and proposes that the new selective TLR4 antagonist aptamer (ApTOLL) may be a promising drug candidate for the treatment of MS and eventually, other demyelinating diseases. Indeed, we not only reveal a possible neuroprotective activity of this antagonist by limiting the inflammatory response but also, by promoting OPC differentiation and myelin formation.

Immunohistochemistry showed TLR4-expressing cells in demyelinating human MS lesions. This result had not yet surfaced despite previous studies such as those based on the RNAseq technology [13, 68]. The distribution of TLR4-positive elements was different in the different histopathological type of lesions: while they were abundant in active lesions (even more than the abundant inflammatory infiltrating cells), these elements drastically reduced their number in the lesions with chronic aspect. Furthermore, the morphology of TLR4-positive elements also varied according to the type of lesion. In chronic lesions, this morphology suggested elements of a neural (i.e. oligodendroglial), very similar to the FGFR1^{+}-OPCs in the periplaque of chronic-active lesions [8]. However, in our present work the TLR4^{+}-cells were almost circumscribed to the core of demyelinating lesions.

Based on the presence of TLR4-positive cells in these lesions of MS patients, we evaluated the potential to use an aptamer to inhibit the activation of the TLR4 signaling. Aptamers are considered candidates for inclusion in therapeutics due to their high affinity and specificity, as well as their advantages over conventional drugs or antibodies (safety, stability, *in vitro* selection, ability to be modified without structural alterations, production costs, etc) [30, 31]. In the present study we have used ApTOLL, an aptamer specifically developed to antagonize TLR4. This aptamer has been shown to be effective in other models of pathology such as ischemic stroke and myocardial infarction [14, 60]. ApTOLL single injection resulted in a significant recovery of clinical symptoms in the EAE model, which was associated with increased myelin and axonal preservation.

In EAE lesions, the aptamer notably reduces the number of microglial cells and TLR4-expressing cells, which could be due to i) the blockage of the membrane binding site and thereby preventing its activation by other ligands, or to ii) the internalization of the receptor once it is antagonized, as proposed previously [55, 71]. The correlation between

the activation of this receptor and microglial behavior might suggest that TLR4 blockade dampens microglial activation and therefore, the inflammatory process [37, 75]. However, those cells that remain active could be participating in phagocytic functions of myelin or axonal debris [59], which is also considered as a necessary process for proper remyelination [16, 41]. Hence, the specific antagonism of TLR4 by ApTOLL but not its complete depletion may produce a remarkable clinical improvement, related to the modulation of an excessively strong immune response, preventing tissue damage. Interestingly, the therapeutic use of TLR4 humans is currently being studied in clinical trials in acute ischemic stroke (NCT04734548) and COVID-19 (NCT05293236) patients and has recently demonstrated good safety and pharmacokinetic properties in healthy volunteers [27].

The role of ApTOLL does not seem to be reduced to its effect on microglia cells and thus on the inflammatory component. Therefore, we have observed a remarkable effect on the elements involved in the remyelination process, that is, on OPCs. This effect goes beyond the fact that ApTOLL decreases inflammatory conditions, to which elements of the oligodendroglial lineage are particularly sensitive [36, 37, 63, 75]. In a non-inflammatory demyelinating scenario, the cuprizone model, the treatment with ApTOLL significantly promoted the number of OPCs and mature oligodendrocytes and myelin distribution. All together reflected acceleration of spontaneous remyelination. In other words, the results observed in the cuprizone model would indicate that the ApTOLL effect is not only translated into an improvement of the survival conditions of the OPCs but also into a proliferation of these cells. To demonstrate this, we used primary cultures of OPCs. This effect of the aptamer would not be minor since it has been demonstrated that, for successful remyelination, quiescent OPCs should proliferate and properly recruited towards areas of demyelination [5, 11, 51] (for a recent review on this specific subject, see [18, 62]).

To provide benefits, it is not only important to increase the number of OPCs, but it is also necessary for them to differentiate towards myelinating phenotypes. It has been argued that the proliferation and differentiation of OPCs are sequential events that cannot take place simultaneously [56]. However, in our present study there was clear evidence of ApTOLL treatment increasing both the number of mature oligodendrocytes and ensheathed axons after a demyelinating insult as well as enhanced myelin formation *ex vivo*. These results would be in line with others that also show that the proliferation of OPCs and the maturation process can coexist [25, 48, 49, 69, 72]. The present data from human adult OPCs strongly support that this would also be the case on human MS. In spite of the remarkable heterogeneity of OPCs recently demonstrated [6, 28, 29, 42], the

present observations suggests that ApTOLL effects on these cells, do not vary according to age or species, which would be very relevant for the future design of clinical trials.

Together, our current findings suggest a new therapeutic approach for the treatment of inflammatory and demyelinating diseases like MS. The molecular nature of the aptamer, ApTOLL, specifically blocking TLR4 exerting a clear anti-inflammatory effect as well as an indirect/direct neuroprotective and remyelinating effect confers advantages over other compounds, and also has a good safety profile, as demonstrated in the First-in-Human study [27]. This opens the door to future clinical studies with this aptamer in MS human trials.

References

1. Andersson A, Covacu R, Sunnemark D, Danilov AI, Dal Bianco A, Khademi M et al (2008) Pivotal advance: HMGB1 expression in active lesions of human and experimental multiple sclerosis. J Leukoc Biol. 84:1248-55. https://doi.org/10.1189/jlb.1207844.
2. Baufeld C, O'Loughlin E, Calcagno N, Madore C, Butovsky O (2018) Differential contribution of microglia and monocytes in neurodegenerative diseases. J Neural Transm. 125:809-826. https://doi.org/10.1007/s00702-017-1795-7.
3. Birgbauer E, Rao TS, Webb M (2004) Lysolecithin induces demyelination in vitro in a cerebellar slice culture system. J Neurosci Res. 78:157-66. https://doi.org/10.1002/jnr.20248.
4. Block ML, Zecca L, Hong JS (2007) Microglia-mediated neurotoxicity: uncovering the molecular mechanisms. Nat Rev Neurosci. 8:57-69. https://doi.org/10.1038/nrn2038.
5. Boyd A, Zhang H, Williams A (2013) Insufficient OPC migration into demyelinated lesions is a cause of poor remyelination in MS and mouse models. Acta Neuropathol. 125:841-59. https://doi.org/10.1007/s00401-013-1112-y.
6. Bribián A, Medina-Rodríguez EM, Josa-Prado F, García-Álvarez I, Machín-Díaz I, Esteban PF et al (2020) Functional heterogeneity of mouse and human brain OPCs: relevance for preclinical studies in multiple sclerosis. J Clin Med. 9:1681. https://doi.org/10.3390/jcm9061681.
7. Bsibsi M, Ravid R, Gveric D, van Noort JM (2002) Broad expression of Toll-like receptors in the human central nervous system. J Neuropathol Exp Neurol. 61:1013-21. https://doi.org/10.1093/jnen/61.11.1013.
8. Clemente D, Ortega MC, Arenzana FJ, de Castro F (2011) FGF-2 and Anosmin-1 are selectively expressed in different types of multiple sclerosis lesions. J Neurosci. 31:14899-909. https://doi.org/10.1523/JNEUROSCI.1158-11.2011.
9. Colton CA (2009) Heterogeneity of microglial activation in the innate immune response in the brain. J Neuroimmune Pharmacol. 4:399-418. https://doi.org/10.1007/s11481-009-9164-4.
10. Constantinescu CS, Farooqi N, O'Brien K, Gran B (2011) Experimental autoimmune encephalomyelitis (EAE) as a model for multiple sclerosis (MS). Br J Pharmacol. 164:1079-1106. https://doi.org/10.1111/j.1476-5381.2011.01302.x.

11. de Castro F, Bribián A, Ortega MC (2013) Regulation of oligodendrocyte precursor migration during development, in adulthood and in pathology. Cell Mol Life Sci. 70:4355-68. https://doi.org/10.1007/s00018-013-1365-6.

12. Dincman TA, Beare JE, Ohri SS, Whittemore SR (2012) Isolation of cortical mouse oligodendrocyte precursor cells. J Neurosci Methods. 209:219-26. https://doi.org/10.1016/j.jneumeth.2012.06.017.

13. Elkjaer ML, Frisch T, Reynolds R, Kacprowski T, Burton M, Kruse TA et al (2019) Molecular signature of different lesion types in the brain white matter of patients with progressive multiple sclerosis. Acta Neuropathol Commun. 7:205. https://doi.org/10.1186/s40478-019-0855-7.

14. Fernández G, Moraga A, Cuartero MI, García-Culebras A, Peña-Martínez C, Pradillo JM et al (2018) TLR4-binding DNA aptamers show a protective effect against acute stroke in animal models. Mol Ther. 26:2047-2059. https://doi.org/10.1016/j.ymthe.2018.05.019.

15. Franco-Pons N, Torrente M, Colomina MT, Vilella E (2007) Behavioral deficits in the cuprizone-induced murine model of demyelination/remyelination. Toxicol Lett. 169:205-13. https://doi.org/10.1016/j.toxlet.2007.01.010.

16. Franklin RJ (2002) Why does remyelination fail in multiple sclerosis? Nat Rev Neurosci. 3:705-14. https://doi.org/10.1038/nrn917.

17. Franklin RJM, Ffrench-Constant C (2017) Regenerating CNS myelin - from mechanisms to experimental medicines. Nat Rev Neurosci. 18:753-769. https://doi.org/10.1038/nrn.2017.136.

18. Franklin RJM, Frisén J, Lyons DA (2021) Revisiting remyelination: Towards a consensus on the regeneration of CNS myelin. Semin Cell Dev Biol. 116:3-9. https://doi.org/10.1016/j.semcdb.2020.09.009.

19. Gambuzza M, Licata N, Palella E, Celi D, Foti Cuzzola V, Italiano D et al (2011) Targeting Toll-like receptors: emerging therapeutics for multiple sclerosis management. J Neuroimmunol. 239:1-12. https://doi.org/10.1016/j.jneuroim.2011.08.010.

20. Gholamzad M, Ebtekar M, Ardestani MS, Azimi M, Mahmodi Z, Mousavi MJ et al (2019) A comprehensive review on the treatment approaches of multiple sclerosis: currently and in the future. Inflamm Res. 68:25-38. https://doi.org/10.1007/s00011-018-1185-0.

21. Green AJ, Gelfand JM, Cree BA, Bevan C, Boscardin WJ, Mei F et al (2017) Clemastine fumarate as a remyelinating therapy for multiple sclerosis (ReBUILD): a randomised, controlled, double-blind, crossover trial. Lancet. 390:2481-2489. https://doi.org/10.1016/S0140-6736(17)32346-2.

22. Gudi V, Moharregh-Khiabani D, Skripuletz T, Koutsoudaki PN, Kotsiari A, Skuljec J et al (2009) Regional differences between grey and white matter in cuprizone induced demyelination. Brain Res. 1283:127-38. https://doi.org/10.1016/j.brainres.2009.06.005.

23. Gudi V, Gingele S, Skripuletz T, Stangel M (2014) Glial response during cuprizone-induced de- and remyelination in the CNS: lessons learned. Front Cell Neurosci. 8:73. https://doi.org/10.3389/fncel.2014.00073.

24. Hanisch UK, Kettenmann H (2007) Microglia: active sensor and versatile effector cells in the normal and pathologic brain. Nat Neurosci. 10:1387-94. doi: 10.1038/nn1997.

25. Hardwick LJ, Ali FR, Azzarelli R, Philpott A (2015) Cell cycle regulation of proliferation versus differentiation in the central nervous system. Cell Tissue Res. 359:187-200. https://doi.org/10.1038/nn1997.

26. Hayakawa K, Pham LD, Seo JH, Miyamoto N, Maki T, Terasaki Y et al (2016) CD200 restrains macrophage attack on oligodendrocyte precursors via toll-like receptor 4 downregulation. J Cereb Blood Flow Metab. 36:781-93. https://doi.org/10.1177/0271678X15606148.

27. Hernández-Jiménez M, Martín-Vílchez S, Ochoa D, Mejía-Abril G, Román M, Camargo-Mamani P et al (2022) First-in-human phase I clinical trial of a TLR4-binding DNA aptamer, ApTOLL: safety and pharmacokinetics in healthy volunteers. Mol Ther Nucleic Acids. 28:124-135. https://doi.org/10.1016/j.omtn.2022.03.005.

28. Hilscher MM, Langseth CM, Kukanja P, Yokota C, Nilsson M, Castelo-Branco G (2022) Spatial and temporal heterogeneity in the lineage progression of fine oligodendrocyte subtypes. BMC biology. 20:122. https://doi.org/10.1186/s12915-022-01325-z.

29. Jäkel S, Agirre E, Mendanha Falcão A, van Bruggen D, Lee KW, Knuesel I et al (2019) Altered human oligodendrocyte heterogeneity in multiple sclerosis. Nature. 566:543-547. https://doi.org/10.1038/s41586-019-0903-2.

30. Kanwar JR, Roy K, Maremanda NG, Subramanian K, Veedu RN, Bawa R et al (2015) Nucleic acid-based aptamers: applications, development and clinical trials. Curr Med Chem. 22:2539–2557. https://doi.org/10.2174/0929867322666150227144909.

31. Keefe AD, Pai S, Ellington A (2010) Aptamers as therapeutics. Nat Rev Drug Discov. 9:537–550. https://doi.org/10.1038/nrd3141.

32. Kerfoot SM, Long EM, Hickey MJ, Andonegui G, Lapointe BM, Zanardo RC et al (2004) TLR4 contributes to disease-inducing mechanisms resulting in central nervous system autoimmune disease. J Immunol. 173:7070-7. https://doi.org/10.4049/jimmunol.173.11.7070.

33. Kipp M, Clarner T, Dang J, Copray S, Beyer C (2009) The cuprizone animal model: new insights into an old story. Acta Neuropathol. 118:723-36. https://doi.org/10.1007/s00401-009-0591-3.

34. Kremer D, Küry P, Dutta R (2015) Promoting remyelination in multiple sclerosis: current drugs and future prospects. Mult Scler. 21:541-9. https://doi.org/10.1177/1352458514566419.

35. Lassmann H, Brück W, Lucchinetti CF (2007) The immunopathology of multiple sclerosis: an overview. Brain Pathol. 17:210-8. https://doi.org/10.1111/j.1750-3639.2007.00064.x.

36. Lehnardt S, Massillon L, Follett P, Jensen FE, Ratan R, Rosenberg PA et al (2003) Activation of innate immunity in the CNS triggers neurodegeneration through a Toll-like receptor 4-dependent pathway. Proc Natl Acad Sci U S A. 100:8514-9. https://doi.org/10.1073/pnas.1432609100.

37. Li JY, Liu Y, Gao XX, Gao X, Cai H (2014) TLR2 and TLR4 signaling pathways are required for recombinant Brucella abortus BCSP31-induced cytokine production, functional upregulation of mouse macrophages, and the Th1 immune response in vivo and in vitro. Cell Mol Immunol. 11:477-94. https://doi.org/10.1038/cmi.2014.28.

38. Liu T, Zhang L, Joo D, Sun SC (2017) NF-κB signaling in inflammation. Sig Transduct Target Ther. 2:17023. https://doi.org/10.1038/sigtrans.2017.23.

39. Lloyd AF, Miron VE (2019) The pro-remyelination properties of microglia in the central nervous system. Nat Rev Neurol. 15:447–458. https://doi.org/10.1038/s41582-019-0184-2.

40. Lu YC, Yeh WC, Ohashi PS (2008) LPS/TLR4 signal transduction pathway. Cytokine. 42:145-151. https://doi.org/10.1016/j.cyto.2008.01.006.

41. Lubetzki C, Zalc B, Williams A, Stadelmann C, Stankoff B (2020) Remyelination in multiple sclerosis: from basic science to clinical translation. Lancet Neurol. 19:678-688. https://doi.org/10.1016/S1474-4422(20)30140-X.

42. Marques S, Zeisel A, Codeluppi S, van Bruggen D, Mendanha Falcão A, Xiao L et al (2016) Oligodendrocyte heterogeneity in the mouse juvenile and adult central nervous system. Science. 352:1326-1329. https://doi.org/10.1126/science.aaf6463.

43. Matsushima GK, Morell P (2001) The neurotoxicant, cuprizone, as a model to study demyelination and remyelination in the central nervous system. Brain Pathol. 11:107-16. https://doi.org/10.1111/j.1750-3639.2001.tb00385.x.

44. Medina-Rodríguez EM, Arenzana FJ, Pastor J, Redondo M, Palomo V, García de Sola R et al (2013) Inhibition of endogenous phosphodiesterase 7 promotes oligodendrocyte precursor differentiation and survival. Cell Mol Life Sci. 70:3449-62. https://doi.org/10.1007/s00018-013-1340-2.

45. Medina-Rodríguez EM, Bribián A, Boyd A, Palomo V, Pastor J, Lagares A et al (2017) Promoting in vivo remyelination with small molecules: a neuroreparative pharmacological treatment for Multiple Sclerosis. Sci Rep. 7:43545. https://doi.org/10.1038/srep43545.

46. Medzhitov R (2001) Toll-like receptors and innate immunity. Nat Rev Immunol. 1:135-45. https://doi.org/10.1038/35100529.

47. Melero-Jerez C, Alonso-Gómez A, Moñivas E, Lebrón-Galán R, Machín-Díaz I, de Castro F et al (2020) The proportion of myeloid-derived suppressor cells in the spleen is related to the severity of the clinical course and tissue damage extent in a murine model of multiple sclerosis. Neurobiol Dis. 140:104869. https://doi.org/10.1016/j.nbd.2020.104869.

48. Melero-Jerez C, Fernández-Gómez B, Lebrón-Galán R, Ortega MC, Sánchez-de Lara I, Ojalvo AC et al (2021) Myeloid-derived suppressor cells support remyelination in a murine model of multiple sclerosis by promoting oligodendrocyte precursor cell survival, proliferation, and differentiation. Glia. 69:905-924. https://doi.org/10.1002/glia.23936.

49. Miron VE, Boyd A, Zhao JW, Yuen TJ, Ruckh JM, Shadrach JL et al (2013) M2 microglia and macrophages drive oligodendrocyte differentiation during CNS remyelination. Nat Neurosci. 16:1211-1218. https://doi.org/10.1038/nn.3469.

50. Moliné-Velázquez V, Cuervo H, Vila-Del Sol V, Ortega MC, Clemente D, de Castro F (2011) Myeloid-derived suppressor cells limit the inflammation by promoting T

lymphocyte apoptosis in the spinal cord of a murine model of multiple sclerosis. Brain Pathol. 21:678-91. https://doi.org/10.1111/j.1750-3639.2011.00495.x.

51. Moyon S, Dubessy AL, Aigrot MS, Trotter M, Huang JK, Dauphinot L et al (2015) Demyelination causes adult CNS progenitors to revert to an immature state and express immune cues that support their migration. J Neurosci. 35:4-20. https://doi.org/10.1523/JNEUROSCI.0849-14.2015.

52. Oh J, Vidal-Jordana A, Montalban X (2018) Multiple sclerosis: clinical aspects. Curr Opin Neurol. 31:752-759. https://doi.org/10.1097/WCO.0000000000000622.

53. Okun E, Griffioen KJ, Lathia JD, Tang SC, Mattson MP, Arumugam TV (2009) Toll-like receptors in neurodegeneration. Brain Res Rev. 59:278-92. https://doi.org/10.1016/j.brainresrev.2008.09.001.

54. Orihuela R, McPherson CA, Harry GJ (2016) Microglial M1/M2 polarization and metabolic states. Br J Pharmacol. 173(4):649-65. https://doi.org/10.1111/bph.13139.

55. Perkins DJ, Richard K, Hansen AM, Lai W, Nallar S, Koller B et al (2018) Autocrine-paracrine prostaglandin E2 signaling restricts TLR4 internalization and TRIF signaling. Nat Immunol. 19:1309-1318. https://doi.org/10.1038/s41590-018-0243-7.

56. Plemel JR, Manesh SB, Sparling JS, Tetzlaff W (2013) Myelin inhibits oligodendroglial maturation and regulates oligodendrocytic transcription factor expression. Glia. 61:1471-87. https://doi.org/10.1002/glia.22535.

57. Poltorak A, He X, Smirnova I, Liu MY, Van Huffel C, Du X et al (1998) Defective LPS signaling in C3H/HeJ and C57BL/10ScCr mice: mutations in TLR4 gene. Science. 282:2085–2088. https://doi.org/10.1126/science.282.5396.2085.

58. Praet J, Guglielmetti C, Berneman Z, Van der Linden A, Ponsaerts P (2014) Cellular and molecular neuropathology of the cuprizone mouse model: clinical relevance for multiple sclerosis. Neurosci Biobehav Rev. 47:485-505. https://doi.org/10.1016/j.neubiorev.2014.10.004.

59. Rajbhandari L, Tegenge MA, Shrestha S, Ganesh Kumar N, Malik A, Mithal A et al (2014) Toll-like receptor 4 deficiency impairs microglial phagocytosis of degenerating axons. Glia. 62:1982-91. https://doi.org/10.1002/glia.22719.

60. Ramírez-Carracedo R, Tesoro L, Hernandez I, Diez-Mata J, Piñeiro D, Hernandez-Jimenez M et al (2020) Targeting TLR4 with ApTOLL improves heart function in response to coronary ischemia reperfusion in pigs undergoing acute myocardial infarction. Biomolecules. 10:1167. https://doi.org/10.3390/biom10081167.

61. Reynolds R, Roncaroli F, Nicholas R, Radotra B, Gveric D, Howell O (2011) The neuropathological basis of clinical progression in multiple sclerosis. Acta neuropathologica. 122:155–170. https://doi.org/10.1007/s00401-011-0840-0.

62. Saitoh SS, Tanabe S, Muramatsu R (2022) Circulating factors that influence the central nervous system remyelination. Curr Opin Pharmacol. 62:130-136. https://doi.org/10.1016/j.coph.2021.12.001.

63. Schonberg DL, Popovich PG, McTigue DM (2007) Oligodendrocyte generation is differentially influenced by toll-like receptor (TLR) 2 and TLR4-mediated intraspinal macrophage activation. J Neuropathol Exp Neurol. 66:1124-35. https://doi.org/10.1097/nen.0b013e31815c2530.

64. Sim FJ, Zhao C, Penderis J, Franklin RJ (2002) The age-related decrease in CNS remyelination efficiency is attributable to an impairment of both oligodendrocyte progenitor recruitment and differentiation. J Neurosci. 22:2451-9. https://doi.org/10.1523/JNEUROSCI.22-07-02451.2002.

65. Skripuletz T, Lindner M, Kotsiari A, Garde N, Fokuhl J, Linsmeier F et al (2008) Cortical demyelination is prominent in the murine cuprizone model and is strain-dependent. Am J Pathol. 172:1053-61. https://doi.org/10.2353/ajpath.2008.070850.

66. Taylor DL, Pirianov G, Holland S, McGinnity CJ, Norman AL, Reali C et al (2010) Attenuation of proliferation in oligodendrocyte precursor cells by activated microglia. J Neurosci Res. 88:1632-44. https://doi.org/10.1002/jnr.22335.

67. Trapp BD, Nave KA (2008) Multiple sclerosis: an immune or neurodegenerative disorder? Annu Rev Neurosci. 31:247-69. https://doi.org/10.1146/annurev.neuro.30.051606.094313.

68. van Wageningen TA, Gerrits E, Brouwer N, Brevé JJP, Geurts JJG, Eggen BJL et al (2002) Distinct gene expression in demyelinated white and grey matter areas of patients with multiple sclerosis. Brain Commun. 4:fcac005. https://doi.org/10.1093/braincomms/fcac005.

69. Wu X, Qu X, Zhang Q, Dong F, Yu H, Yan C et al (2014) Quercetin promotes proliferation and differentiation of oligodendrocyte precursor cells after oxygen/glucose deprivation-induced injury. Cell Mol Neurobiol. 34:463-71. https://doi.org/10.1007/s10571-014-0030-4.

70. Young K, Morrison H (2018) Quantifying microglia morphology from photomicrographs of immunohistochemistry prepared tissue using ImageJ. J Vis Exp. (136):57648. https://doi.org/10.3791/57648.

71. Zanoni I, Ostuni R, Marek LR, Barresi S, Barbalat R, Barton GM et al (2011) CD14 controls the LPS-induced endocytosis of Toll-like receptor 4. Cell. 147:868-80. https://doi.org/10.1016/j.cell.2011.09.051.

72. Zhang J, Zhang ZG, Li Y, Ding X, Shang X, Lu M et al (2015) Fingolimod treatment promotes proliferation and differentiation of oligodendrocyte progenitor cells in mice with experimental autoimmune encephalomyelitis. Neurobiol Dis. 76:57-66. https://doi.org/10.1016/j.nbd.2015.01.006.

73. Zhang Y, Han J, Wu M, Xu L, Wang Y, Yuan W et al (2019) Toll-Like Receptor 4 promotes Th17 lymphocyte infiltration via CCL25/CCR9 in pathogenesis of experimental autoimmune encephalomyelitis. J Neuroimmune Pharmacol. 14:493-502. https://doi.org/10.1007/s11481-019-09854-1.

74. Zhang ZM, Wang YC, Chen L, Li Z (2019) Protective effects of the suppressed NF-κB/TLR4 signaling pathway on oxidative stress of lung tissue in rat with acute lung injury. Kaohsiung J Med Sci. 35:265-276. https://doi.org/10.1002/kjm2.12065.

75. Zhao Y, Zhao Y, Zhang M, Zhao J, Ma X, Huang T et al (2016) Inhibition of TLR4 Signalling-induced inflammation attenuates secondary injury after diffuse axonal injury in rats. Mediators Inflamm. 2016:4706915. https://doi.org/10.1155/2016/4706915.

76. Zhou J, Rossi J (2017) Aptamers as targeted therapeutics: current potential and challenges. Nat Rev Drug Discov. 16:181-202. https://doi.org/10.1038/nrd.2016.199.

Acknowledgements

This work was supported by grant IND2018/BMD-9751 (Programa de Doctorados Industriales, *Comunidad de Madrid*, Spain), SAF2016-77575-R (Spanish Ministerio de Economía, Industria y Competitividad-MINECO), and the contract for technological support ApTLR2019-PC-MS-001 (AptaTargets, S.L., Spain) to FdC. BF-G is currently hired by Aptatargets S.L., PG-M is hired under PEJ-2020-AI/BMD-18541 de la Comunidad de Madrid, Spain (associated with the youth guarantee fund to FdC), SN had a predoctoral contract from the UCLM and was hired under SAF2012-40023, SAF2016-77575-R, RD12-0032/0012 and RD16-0015/0019 (Spanish Ministerio de Economía, Industria y Competitividad-MINECO) and IND2018/BMD-9751, YL has been contracted under ReTics and SAF (to FdC). We thank David Segarra and Mª Eugenia Zarabozo (AptaTargets S.L.) for their constant technological support, Laude Garmendia for her indispensable constant help at the animal facility (Instituto Cajal-CSIC), including the extra effort during Covid-19 pandemics, Profs María Ángeles Moro (Centro Nacional de Investigaciones Cardiovasculares Carlos III, Madrid and Universidad Complutense de Madrid, Spain) and Ignacio Lizasoaín (Universidad Complutense de Madrid, Spain) for lending us the TLR4 *knockout* mice, and the former GNDe member Dr. Carolina Melero-Jerez (currently working at JazzPharma, Spain) for the initial training of BF-G on EAE animal model and different techniques at the laboratory. Human samples were supplied by the UK Multiple Sclerosis Tissue Bank, funded by the Multiple Sclerosis Society of Great Britain and Northern Ireland (registered charity 207495).

FIGURE LEGENDS

Fig 1. Characterization and expression of TLR4 in human brain demyelinated lesions of MS patients. Representative images of cortical lesions from controls and MS patients with demyelinating lesions surrounded in white (**a, e, i**). Characterization of demyelinating lesion type by the presence of the HLA-DR marker. No accumulation is observed in the control (**b**) while HLA^+ cells are abundant in active plaques (**f**) but scarce in the core of chronic lesions (**j**). MS patients showed TLR4 expression in demyelinated lesions while in control tissue it was not observed (**c, g, k**). Magnifications of TLR4-labeled cells (**d, h, i**). Scale bar, 500 µm in **a**, **e** and **i**; 250 µm in **b-c, f-g, j-k**; and 50 µm in **d, h** and **i**.

Fig 2. ApTOLL improves the symptomatology of EAE mice, protecting them from demyelination. a Follow-up of the clinical course in animals treated at the onset of symptoms with a single dose of ApTOLL (0.91mg/Kg, n=13) relative to the mice that received the vehicle alone (Veh, n=6). **b** EC staining of spinal cord sections in which the white arrows indicate lesions. **c** Quantification of the demyelinated areas within the white matter. **d** Representative images showing the demyelinated areas (indicated by the white dashed lines) characterized by the lack of myelin (MBP) and neurofilaments (NHF) in the spinal cord lesions, and the oligodendrocyte labeling at different stages of maturation: Olig2 for all lineage (red), PDGFRα for immature cells (green), and CC1 for mature cells (gray). **e-g** Graphs showing the percentage area of MBP (**e**), NFH (**f**) and oligodendrocytes (**g**) in EAE mice. In ApTOLL-treated animals there was an increase in the extension of each marker. Scale bar, 200 µm in **b** and **d**. The results of the Student's *t*-test are represented as: *p <0.05; **p <0.01, and ***p <0.001.

Fig 3. $TLR4^{-/-}$ animals show no improvement with ApTOLL treatment, indicating the specificity of its effects. a The clinical course of the animals did not differ between EAE-Veh animals (n=6) and the $TLR4^{-/-}$ EAE mice treated with (n=6) or without ApTOLL (n=5), although ApTOLL significantly reduced the intensity of the symptoms in the WT EAE mice (n=13). **b-c** Images and quantification of lesion zones within the white matter in each experimental group, the white arrows indicating the areas of demyelination. **d-f** Representative images (**d**), and the quantification of myelin (**e**) and axons (**f**) in the different mouse genotypes. **g-i** Study of the oligodendroglial lineage in $TLR4^{-/-}$ EAE mice. Scale bar, 200 µm in **b**, **d** and **g**. The results of one-way ANOVA with a Dunn's or Tukey's *post hoc* test are represented as: *p <0.05; **p <0.01, and ***p <0.001. The significant results of the Student's *t*-test comparing pairs of groups are indicated as: ## p <0.01.

Fig 4. Microglia and TLR4 expression are reduced in spinal cord lesions of EAE-ApTOLL mice. a Representative images and magnifications of the lesions showing the microglial (green) and TLR4 (magenta) labelling. **b-d** Quantification of the microglial cells in the spinal cord (**b**), the total number of TLR4-expressing cells within the lesion (c) and of the microglial cells that colocalize with this receptor (**d**). A significant reduction in all these parameters was observed following ApTOLL treatment. **e** The expression of TLR4 directly correlates with microglia (Iba1). Scale bar, 60 μm in **a** and 30 μm in magnifications. The Student's *t*-test was used to compare the groups: **p <0.01.

Fig 5. Myelin and oligodendrocytes increase in the CC of CPZ-ApTOLL mice. a Scheme of the experimental procedure. **b** Results from the rotarod assay performed at the end of 6-weeks. Animals that received ApTOLL weekly took longer to fall off the rod than the mice that received the vehicle alone. **c-g** Confocal images of the CC after receiving CPZ for 6 weeks and quantification of the staining for myelin (green, **d**), paranodes (magenta, **e**), OPCs (cyan, **f**) and mature oligodendrocytes (gray, **g**). A significant enhancement in myelin and in the number of oligodendrocytes was observed in CPZ-ApTOLL animals. Scale bar, 60 μm in **c** and 20 μm in Caspr staining. At least 4 mice per group were used and the results of the one-way ANOVA test for multiple comparisons are represented as: *p <0.05; **p <0.01, and ***p <0.001. A Student's *t*-test was used to compare pairs of conditions, represented as: $^{\#}$p <0.05.

Fig 6. ApTOLL enhances murine OPC proliferation and differentiation. a Representative images of OPCs expressing TLR4 (magenta). **b** Images of OPCs labeled for Olig2 (red) and apoptotic TUNEL stained cells (green). **c** There are no differences in the survival of cells under the different conditions. **d** Images showing proliferating cells that express BrdU (green). **e** The proportion of $Olig2^{+}/BrdU^{+}$ increases with both doses of ApTOLL when compared to the vehicle alone. **f** Representative images of differentiated OPCs expressing MBP (green). **g** Graph showing an enhanced number of myelin-forming cells induced by ApTOLL in the culture medium. Arrows indicate double-labeled cells. Scale bar, 20 μm in **a** and 50 μm in **b**, **d** and **f**. At least three independent experiments per experimental condition were performed and the results of one-way ANOVA followed by Dunn's or Tukey's *post hoc* test are expressed as: *p <0.05; **p <0.01, and ***p <0.001.

Fig 7. ApTOLL promotes remyelination *ex vivo*. a Scheme of the experimental procedure to maintain cerebellar slices in organotypic culture. **b** Representative images of the parallel fibers (NFH, magenta) present in the cerebellar samples, and of myelin (MBP, green), under the different conditions after exposure to a demyelinating insult with LPC. **c-d** Graphs shows a significant increase in both the total myelin area **(c)** and co-localization with neurofilaments (**d**) in the LPC-lesioned slices treated with ApTOLL. Scale bar, 50 µm in **b** and a minimum of three independent experiments per experimental condition were analyzed. A Student's *t*-test was used and represented as: *p <0.05; **p <0.01, and ***p <0.001.

Fig 8. ApTOLL exerts a direct effect on the differentiation of OPCs from human biopsies. a Representative images of human mature oligodendrocytes expressing CC1 (magenta) and MBP (green). **b-c** Enhanced numbers of mature cells (**b**) and an increase in the area occupied by MBP (**c**) is observed in the presence of ApTOLL. Scale bar, 50 µm in **a**. The results of one-way ANOVA with a Tukey's *post hoc* test are expressed as: ***p <0.001.

Supplementary Fig 1. Dose-response study. a Clinical course of the animals treated with each dose of ApTOLL compared to each vehicle group. There is a significant recovery in the clinical course of EAE after the injection of ApTOLL at the time of the onset of symptoms, both at a dose of 0.91 mg/Kg and 1.82 mg/Kg. **b-c** Demyelinated areas are indicated with white arrows (**b**) and quantified with respect to the white matter area in each experimental group (**c**). The optimal doses for ApTOLL treatment in the murine EAE model of MS are the intermediate ones. **d-e** Images of the different markers in the lesions (dashed white lines): MBP (red), NFH (gray), and Iba1 (green) (**d**). Graphs representing the recovery rate of ApTOLL-treated mice relative to the vehicle group (**e**). **f-g** Magnified images (**f**) and histograms (**g**) of the oligodendrocyte studies at different stages of maturation. The 0.91 mg/Kg dose is optimal for ApTOLL-treatment in EAE. Scale bar, 200 µm in **b**, **d** and **f**. EAE-ApTOLL n=6, EAE-Veh n=4, *Sham* n=5 for a dose of 0.45 mg/kg, EAE-ApTOLL n=13, EAE-Veh n=6, *Sham* n=10 for a dose of 0.91 mg/kg; EAE-ApTOLL n=8, EAE-Veh n=7, *Sham* n=8 for a dose of 1.82 mg/Kg; EAE-ApTOLL n=5, EAE-Veh n=4, *Sham:* n=5 for a dose of 3.6 mg/Kg. Results of the one-way ANOVA with a Tukey's *post hoc* test and of the Student's *t*-test for two independent groups are represented as: *p <0.05, **p <0.01, and ***p <0.001.

Supplementary Fig 2. Study of the therapeutic window with the optimal dose of ApTOLL. a Clinical course of the animals treated with ApTOLL at different time

points of the disease relative to their respective vehicle group: onset (EAE-Veh n=6; EAE-ApTOLL n=13), 24h post-onset (EAE-Veh n=4, EAE-ApTOLL n=4) and peak (EAE-Veh n=4, EAE-ApTOLL n=5). **b-c** Representative images of EC staining (b) and the quantification of demyelination relative to their respective vehicle group **(c)**. White arrows indicate lesions. The treatment is more effective when injected at the onset of symptoms. **d-e** Representative images (**d**) and graphical representation of the recovery rate of MBP, NFH and Iba1 relative to the vehicle group (**e**). **f-g** Representative magnification of the oligodendrocyte labeling at different stages of maturation (**f**) and a graph of the oligodendrocyte ratio at different times of injection (**g**). Scale bar, 200 μm in **b**, **d** and **f**, and the results of the one-way ANOVA with a Dunn's or Tukey's *post hoc* test are represented as: *p <0.05, **p <0.01, and ***p <0.001.

Supplementary Fig 3. Morphological changes towards reparative phenotypes in microglia from LPC-lesioned slices that received ApTOLL. **a** Representative images of microglial cells and magnified images of single cells selected randomly from organotypic cerebellar slices exposed to LPC. **b-d** Skeleton analysis of cells shows an increase in the end-point voxels (**b**), branches (**c**) and in their length (**d**) when treated with ApTOLL. The results reveal an activated state in the control condition at 0 dpl and a complex/ramified morphology in ApTOLL treated slices. Scale bar, 50 μm in **a** and 15 μm in magnifications. At least 30 cells were analyzed in a minimum of three independent experiments. The results of the one-way ANOVA are represented as: *p <0.05, and ***p <0.001.

Supplementary Fig 4. a-f The OPC cultures from TLR4$^{-/-}$ mice revealed no differences between any group regarding survival (**a, b**), proliferation (**c, d**) or differentiation (**e, f**). Scale bar, 60 μm in **a**, **c** and **e**, and one-way ANOVA was performed with a Dunn's or Tukey's *post hoc* test.

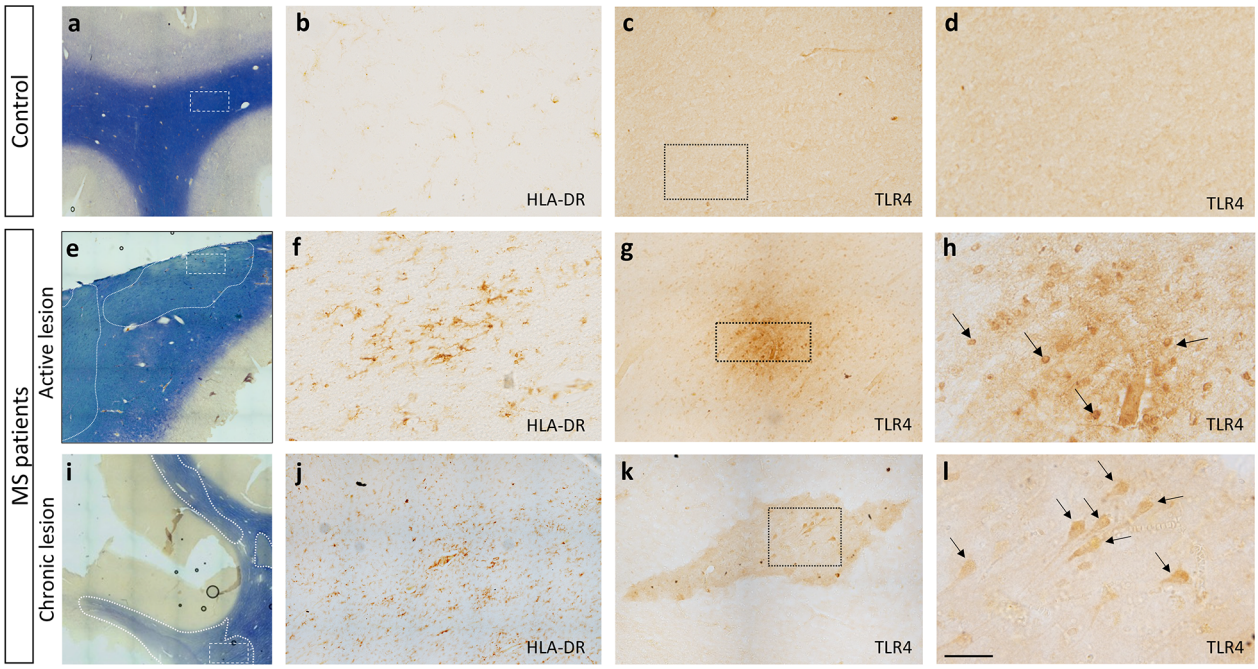
Control
MS patients
Active lesion
Chronic lesion
a
b
HLA-DR
c
TLR4
d
TLR4
e
f
HLA-DR
g
TLR4
h
TLR4
i
j
HLA-DR
k
TLR4
l
TLR4

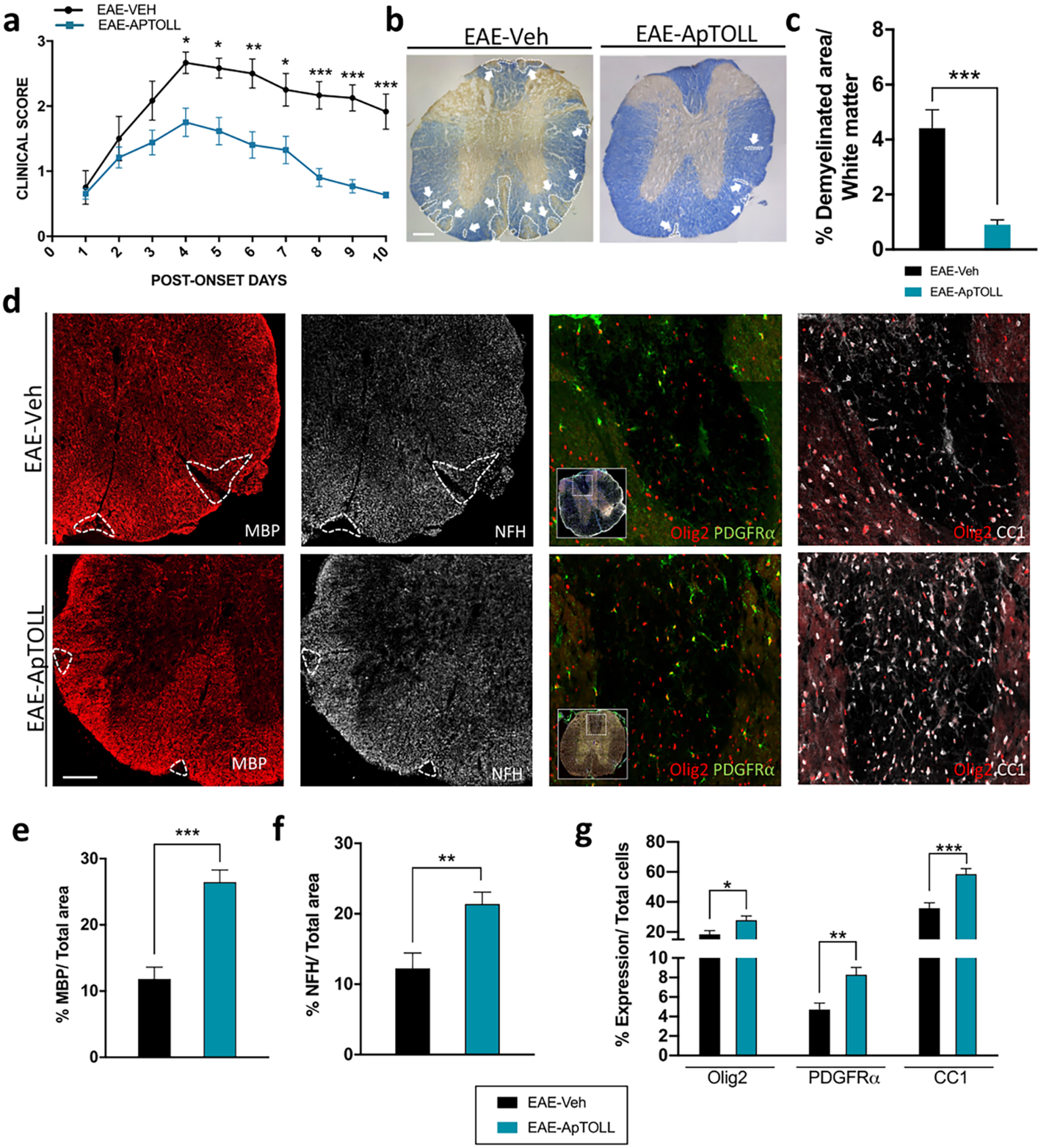
a
EAE-VEH
EAE-APTOLL
CLINICAL SCORE
POST-ONSET DAYS
b
EAE-Veh
EAE-ApTOLL
c
% Demyelinated area/ White matter
EAE-Veh
EAE-ApTOLL
d
EAE-Veh
EAE-ApTOLL
MBP
NFH
Olig2 PDGFRα
Olig2 CC1
e
% MBP/ Total area
f
% NFH/ Total area
g
% Expression/ Total cells
Olig2
PDGFRα
CC1
EAE-Veh
EAE-ApTOLL

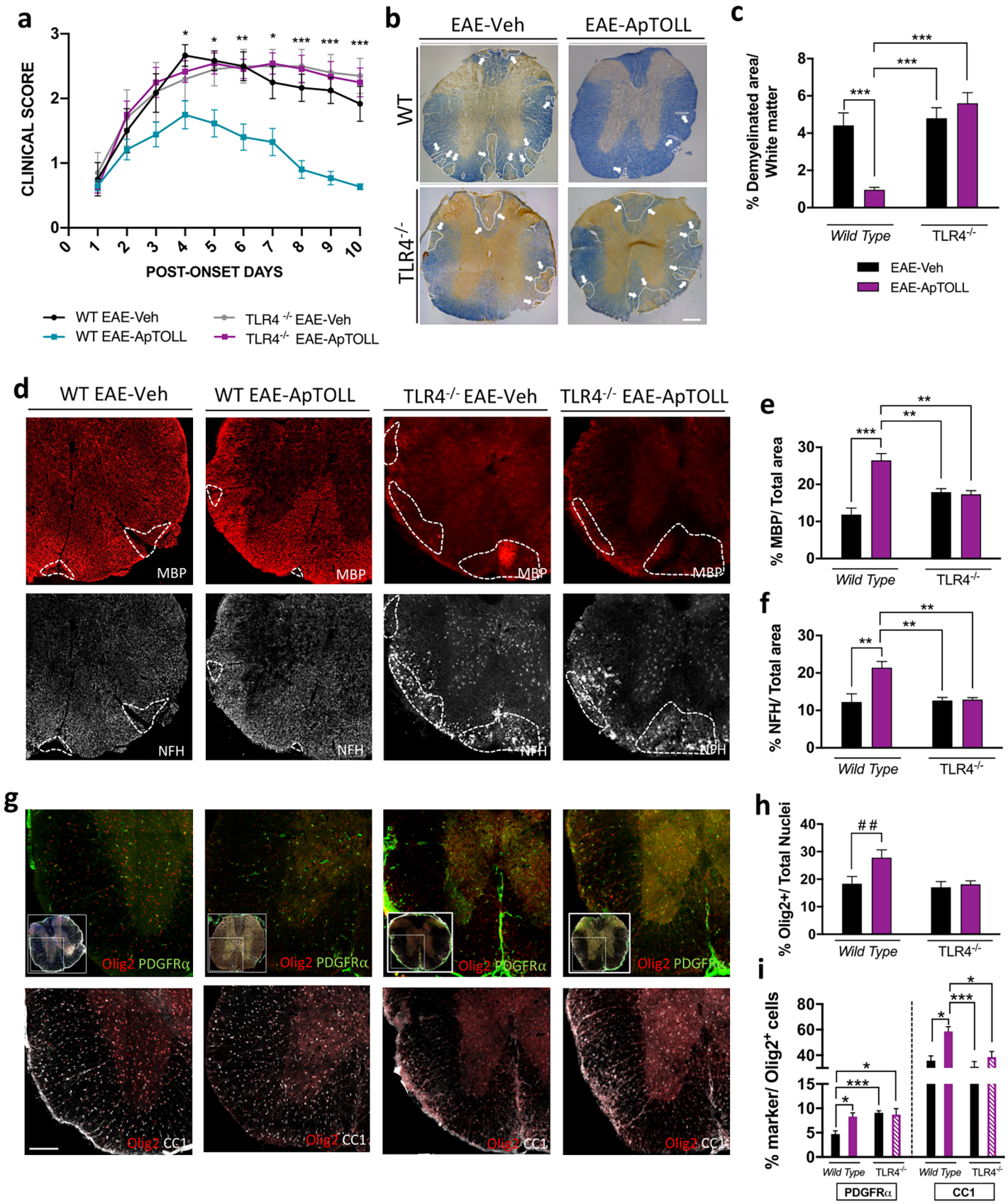
a
CLINICAL SCORE
POST-ONSET DAYS
WT EAE-Veh
WT EAE-ApTOLL
TLR4 -/- EAE-Veh
TLR4-/- EAE-ApTOLL
b
EAE-Veh
EAE-ApTOLL
WT
TLR4-/-
c
% Demyelinated area/ White matter
Wild Type
TLR4-/-
EAE-Veh
EAE-ApTOLL
d
WT EAE-Veh
WT EAE-ApTOLL
TLR4-/- EAE-Veh
TLR4-/- EAE-ApTOLL
MBP
NFH
e
% MBP/ Total area
f
% NFH/ Total area
g
Olig2 PDGFRα
Olig2 CC1
h
% Olig2+/ Total Nuclei
i
% marker/ Olig2+ cells
PDGFRα
CC1

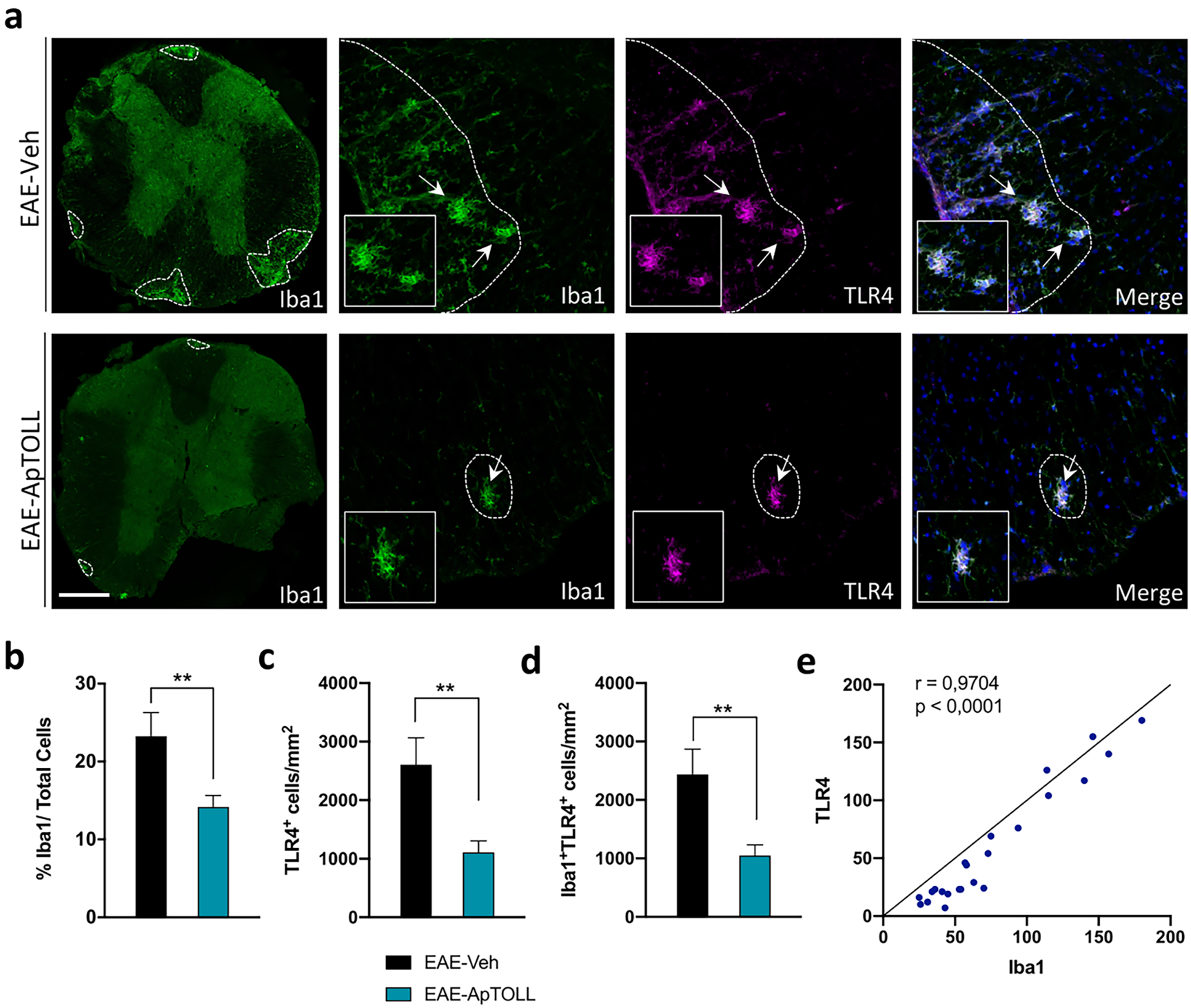
a
EAE-Veh
EAE-ApTOLL
Iba1
Iba1
TLR4
Merge
Iba1
Iba1
TLR4
Merge
b
% Iba1/ Total Cells
**
c
TLR4+ cells/mm2
**
d
Iba1+TLR4+ cells/mm2
**
EAE-Veh
EAE-ApTOLL
e
r = 0,9704
p < 0,0001
TLR4
Iba1

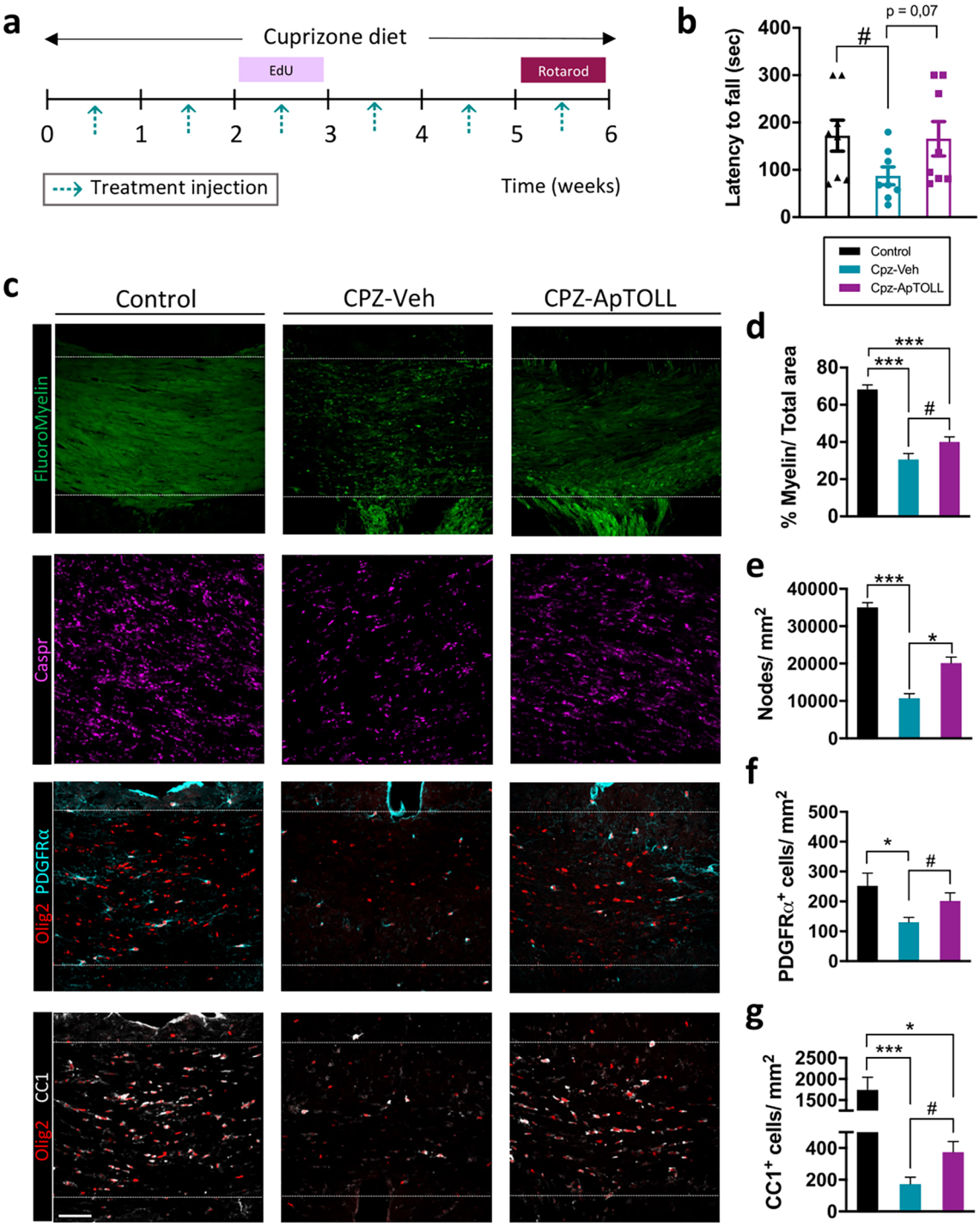
a
Cuprizone diet
EdU
Rotarod
0
1
2
3
4
5
6
Treatment injection
Time (weeks)
b
Latency to fall (sec)
p = 0,07
#
Control
Cpz-Veh
Cpz-ApTOLL
c
Control
CPZ-Veh
CPZ-ApTOLL
FluoroMyelin
Caspr
Olig2 PDGFRα
Olig2 CC1
d
% Myelin/ Total area
***
#
e
Nodes/ mm²
***
*
f
PDGFRα⁺ cells/ mm²
*
#
g
CC1⁺ cells/ mm²
*
***
#

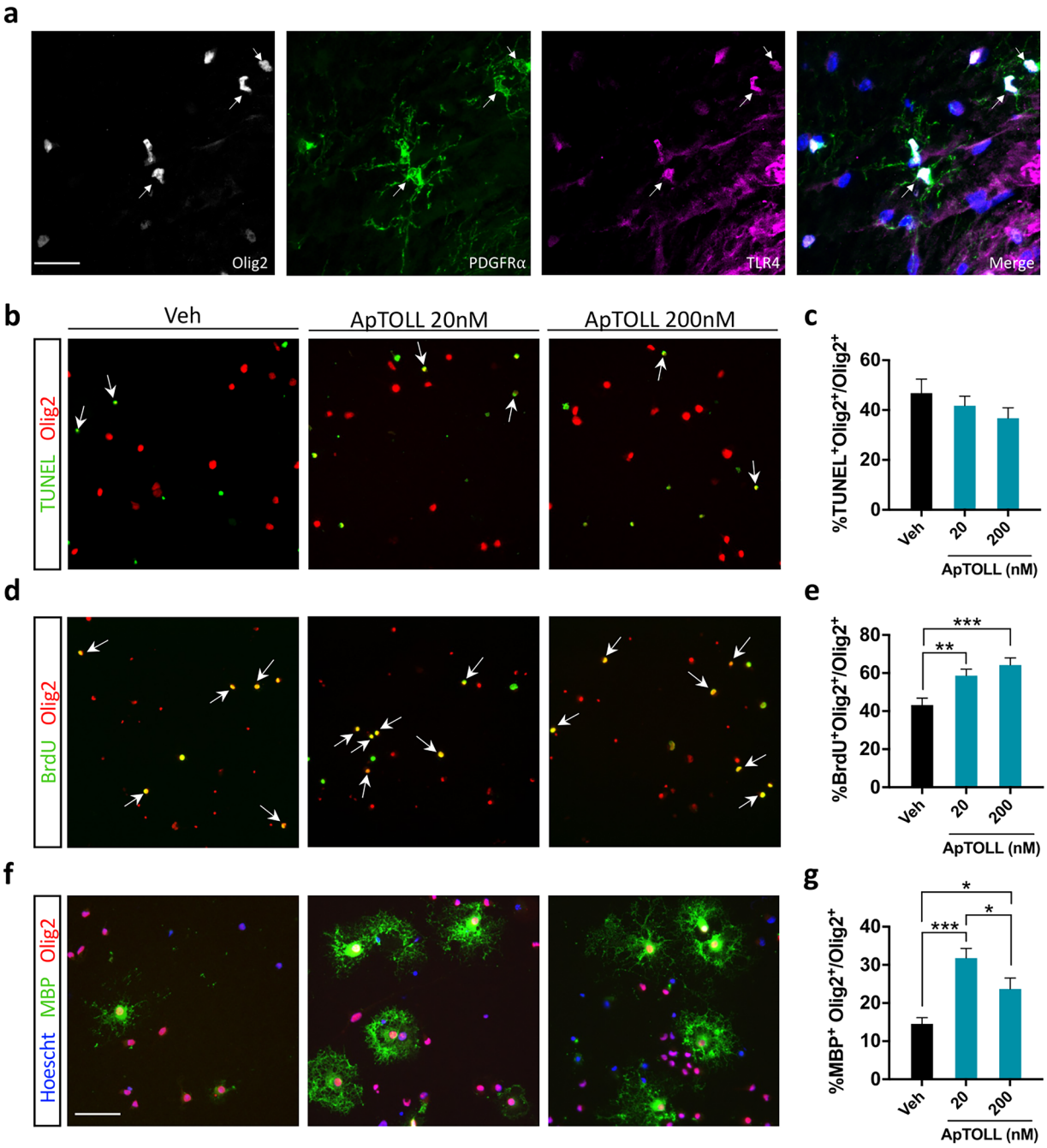
a
Olig2
PDGFRα
TLR4
Merge
b
Veh
ApTOLL 20nM
ApTOLL 200nM
TUNEL Olig2
c
%TUNEL+Olig2+/Olig2+
60
40
20
0
Veh
20
200
ApTOLL (nM)
d
BrdU Olig2
e
%BrdU+Olig2+/Olig2+
80
60
40
20
0
***
**
Veh
20
200
ApTOLL (nM)
f
Hoescht MBP Olig2
g
%MBP+ Olig2+/Olig2+
40
30
20
10
0
*
***
*
Veh
20
200
ApTOLL (nM)

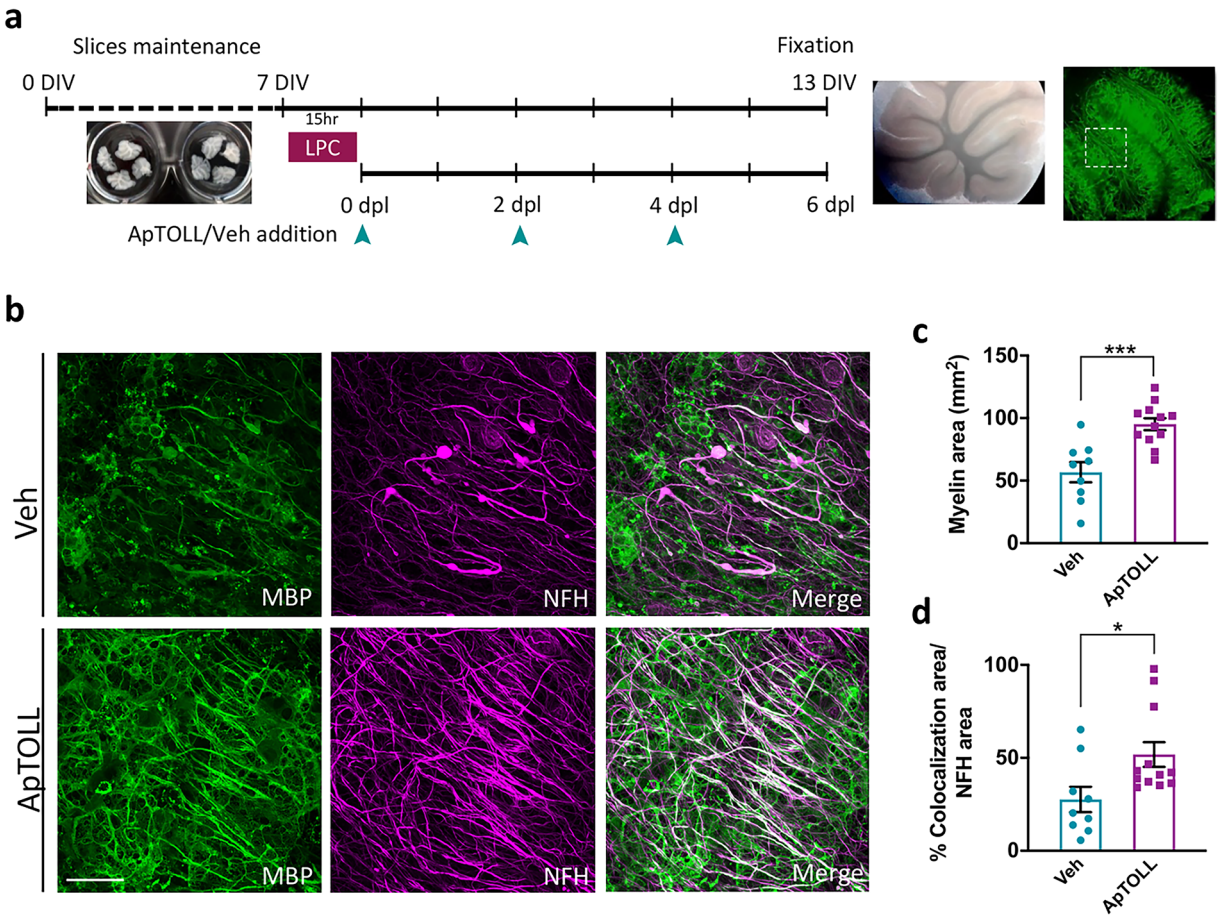
a
Slices maintenance
Fixation
0 DIV
7 DIV
13 DIV
15hr
LPC
0 dpl
2 dpl
4 dpl
6 dpl
ApTOLL/Veh addition
b
Veh
ApTOLL
MBP
NFH
Merge
c
Myelin area (mm²)
150
100
50
0
***
Veh
ApTOLL
d
% Colocalization area/ NFH area
100
50
0
*
Veh
ApTOLL

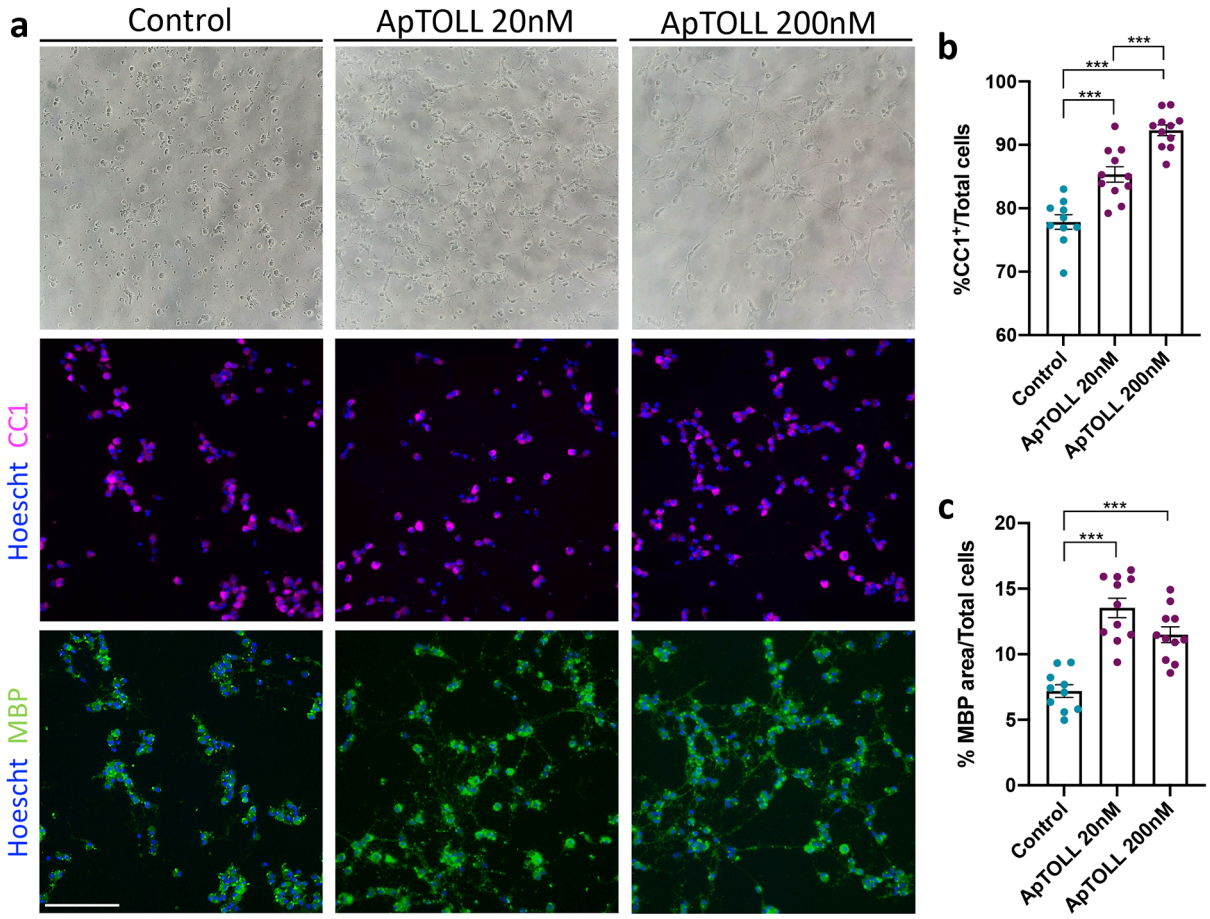
a
Control
ApTOLL 20nM
ApTOLL 200nM
Hoescht CC1
Hoescht MBP
b
%CC1+/Total cells
100
90
80
70
60
***
***
***
Control
ApTOLL 20nM
ApTOLL 200nM
c
% MBP area/Total cells
20
15
10
5
0
***
***
Control
ApTOLL 20nM
ApTOLL 200nM

Table 1. Summary of the human samples analyzed.

Patient	Age (years)/ Sex	Diagnostic	Time *post-mortem* (h)	Disease duration (years)	Cause of death
MS60	55/M	SP	16	43	Aspiration of gastric contents, multiple sclerosis
MS73	80/F	SP	20	50	Bronchopneumonia
MS94	42/F	PP	11	6	Bronchopneumonia, Multiple Sclerosis
MS100	46/M	SP	7	8	Pneumonia
MS115	76/F	SP	21	58	Multiple Sclerosis
MS125	76/F	SP	13	30	Multiple Sclerosis
MS249	69/F	RR	8	42	Thoracic infection, heart failure
MS274	56/M	RR	8	19	Cancer of oesophagus
CO02	85/M	Normal	12	_____	Prostate cancer
CO05	95/F	Normal	10	_____	Bronchopneumonia
CO11	77/M	Normal	26	_____	Carcinoma of the lung metastasised
Co013	73/F	Normal	59	_____	Cancer of oesophagus
Co025	35/M	Normal	22	_____	Carcinoma of the tongue

Abbreviations: MS, Multiple Sclerosis; Co, Control; F, female; M, male; SP, secondary progressive; PP, primary progressive; RR, relapsing remitting.

Use	Antibody	Target	Dilution	Species	Supplier
IHC	NFH	Neurofilaments	1:1000	Rabbit	Abcam
IHC	Iba1	Microglia	1:500	Guinea pig	Synaptic system
IHC	CC1	Mature oligodendrocytes	1:200	Mouse	Millipore
IHC	PDGFRα	OPCs	1:200	Goat	R&D systems
IHC	Caspr	Paranodes	1:900	Rabbit	Abcam
IHC	TLR4	Toll-like receptor 4	1:100	Rat	Santa Cruz
IHC	TLR4	Toll-like receptor 4	1:100	Mouse	Abcam
IHC	HLA-DR	Human leukocyte antigen	1:900	Mouse	ThermoFisher
IHC/ICC	MBP	Myelin	1:500	Rat	Serotec
IHC/ICC	Olig2	Oligodendroglial lineage	1:200	Rabbit	Millipore
ICC	BrdU	Proliferating cells	1:1000	Rat	Abcam

Table 2. List of primary antibodies used

Abbreviations: IHC, immunohistochemistry; ICC, immunocytochemistry; OPCs, oligodendrocyte precursor cells.